

REVIEW

View Article Online
View Journal | View Issue



Cite this: RSC Adv., 2021, 11, 31098

Expanding the PET radioisotope universe utilizing solid targets on small medical cyclotrons

K. J. H. George, ^{ab} S. Borjian, ^e M. C. Cross, ^e J. W. Hicks, ^{ab} P. Schaffer ^{defg} and M. S. Kovacs ^b *^{abc}

Molecular imaging with medical radioisotopes enables the minimally-invasive monitoring of aberrant biochemical, cellular and tissue-level processes in living subjects. The approach requires the administration of radiotracers composed of radioisotopes attached to bioactive molecules, the pairing of which considers several aspects of the radioisotope in addition to the biological behavior of the targeting molecule to which it is attached. With the advent of modern cellular and biochemical techniques, there has been a virtual explosion in potential disease recognition antigens as well as targeting moieties, which has subsequently opened new applications for a host of emerging radioisotopes with well-matched properties. Additionally, the global radioisotope production landscape has changed rapidly, with reactor-based production and its long-defined, large-scale centralized manufacturing and distribution paradigm shifting to include the manufacture and distribution of many radioisotopes via a worldwide fleet of cyclotrons now in operation. Cyclotron-based radioisotope production has become more prevalent given the commercial availability of instruments, coupled with the introduction of new target hardware, process automation and target manufacturing methods. These advances enable sustained, higher-power irradiation of solid targets that allow hospital-based

Received 9th June 2021 Accepted 25th August 2021

DOI: 10.1039/d1ra04480j

rsc.li/rsc-advances

- ^aLawson Health Research Institute, 268 Grosvenor Street, London, ON, N6A 4V2, Canada. E-mail: mkovacs@lawsonimaging.ca
- ^bMedical Biophysics, Western University, 1151 Richmond Street N., London, ON, N6A 5C1, Canada
- ^cMedical Imaging, Western University, 1151 Richmond Street N., London, ON, N6A 5C1, Canada
- dLife Sciences, TRIUMF, 4004 Wesbrook Mall, Vancouver, BC, V6T 2A3, Canada

eARTMS, 301-4475 Wayburn Drive, Burnaby, BC, V5G 4X4, Canada

Radiology, University of British Columbia, 2775 Laurel St, Vancouver, BC, V5Z 1M9, Canada

Chemistry, Simon Fraser University, 8888 University Dr, Burnaby, BC, V5A 1S6, Canada



Keller Joshell Hadassah George obtained her BSc in chemical engineering at the Illinois Institute of Technology in 2013. She then obtained her MESc and PhD at Western University in 2015 and 2019 respectively. She currently holds a Mitacs Accelerate Postdoctoral Fellowship at Western University/ARTMS, and her research focuses on the optimization of separation methods for cyclotron-produced ⁶⁸Ga on solid targets.



Sogol Borjian received a BSc (2005) and MSc (2007) in Polymer Engineering from Amirkabir University of Technology in Tehran, Iran. She then received a PhD (2014) in Organometallic Chemistry from Queen's University in Kingston, ON, where her research focused on developing new palladium catalysts for pharmaceutical applications. She followed with an Industrial Postdoctoral Fellowship in

collaboration with ABB (Zurich) where her research focused on developing novel thin films for selective chemical sensing using micro-optical devices. Sogol joined ARTMS Inc. in 2018 and is currently responsible for managing the Chemistry and Target Production teams, overseeing the development and commercialization of medical radioisotopes used in cancer diagnosis and treatment.

radiopharmacies to produce a suite of radioisotopes that drive research, clinical trials, and ultimately clinical care. Over the years, several different radioisotopes have been investigated and/or selected for radiolabeling due to favorable decay characteristics (i.e. a suitable half-life, high probability of positron decay, etc.), well-elucidated chemistry, and a feasible production framework. However, longer-lived radioisotopes have surged in popularity given recent regulatory approvals and incorporation of radiopharmaceuticals into patient management within the medical community. This review focuses on the applications, nuclear properties, and production and purification methods for some of the most frequently used/emerging positron-emitting, solid-target-produced radioisotopes that can be manufactured using small-to-medium size cyclotrons (≤24 MeV).

Introduction

Positron Emission Tomography (PET) is one of several diagnostic imaging tools used to non-invasively assess metabolic

activity in body tissue. PET scanning is sensitive enough to quantify changes in biological processes, making it an ideal candidate for assessing the efficacy of an early treatment plan or newly developed drugs. PET makes use of radiotracers which permit the visual isolation of metabolic processes within



Michael Cross is a co-founder and COO of ARTMS Inc. where he is responsible for overseeing operational activities, establishing regulatory and clinical strategies, and innovator and research collaborations. Previously Michael was General Manager at the Centre for Probe Development and Commercialization (McMaster University). Michael has over 20 years of healthcare and life science

industry experience. Michael co-founded and was COO/CBO of OncoSec Medical and was also the SVP and co-lead of a \$330 M life sciences venture fund. Michael received his PhD in physiology and MBA from the University of Toronto and was a post-doctoral fellow with the Department of National Defence.



Paul Schaffer obtained his PhD (Chemistry) in 2003 from McMaster University, after which he transitioned to become a Research Associate at McMaster Nuclear Reactor. This was followed by a role of Lead Scientist at GE Global Research. Since 2009, he has served as Associate Laboratory Director, Life Sciences at TRIUMF since 2012. Dr Schaffer is an Associate Professor in Radiology at the

University of British Columbia, an adjunct professor in Chemistry at Simon Fraser University and is affiliated with the Research Center for Nuclear Physics at Osaka University. Dr Schaffer now serves as Chief Technology of ARTMS, Inc.; a spin-off company resulting from his research in large-scale cyclotron-based production of ^{99m}Tc in response to the 2007–2009 supply crises.



Justin Hicks is a research scientist focusing on radiochemistry for molecular imaging applications to investigate pressing biomedical questions. He received a MSc in 99m Tc chemistry under Dr John Valliant at McMaster University (2010). He then completed a PhD on PET tracer development with Drs Alan Wilson and Neil Vasdev at the University of Toronto (2015). Dr Hicks then joined the Lawson

Health Research Institute cyclotron as a radiochemist to translate clinical PERS, followed in 2016 by appointments as a Lawson Scientist and Assistant Professor in Medical Biophysics at Western University.



Michael Kovacs received his PhD (Medicinal Inorganic Chemistry) from the University of British Columbia in 2001. Under an NSERC Industrial Fellowship, he worked at Advanced Cyclotron Systems Inc (ACSI) where he lead research and development work on automated radiochemistry synthesis and cyclotron targetry. He was recruited as a Scientist by the Lawson Health Research Institute in 2003 to

create a PET cyclotron and radiochemistry research program (founded 2010). Dr Kovacs is currently the Director of the Lawson Cyclotron and is Assistant Professor in Medical Imaging and Medical Biophysics at Western University. His research interests include the production and application of metal ions to PET imaging.

specific tissues and cells. These radiotracers are composed of a radioisotope attached to a bioactive molecule (e.g. a small molecule, peptide, antibody, etc.), as demonstrated in Fig. 1. The choice of bioactive targeting molecule mainly depends on the process to be visualized but also on the molecule's ability to incorporate the radioisotope into the chemical structure of the pharmaceutical compound. However, choosing the radioisotope requires consideration of biocompatibility in addition to the assessment of physical and biological half-life suitability for the metabolic process under investigation.²⁻⁴ Over the years, the suitability of several PET radioisotopes for use as tracers has been advanced, along with their unique methods of production.2,5 There are three major methods that can be used to produce radiometals - parent/progeny generators, nuclear reactors and cyclotrons.2 For radioisotope production utilizing cyclotrons, radioisotopes can be produced using gas, liquid, or solid phase targets.2,6 This review will focus on recent advancements in the use of solid targets.

The design of a solid target requires several considerations, and these factors influence its configuration and performance. Targets may be composed entirely of enriched and natural elements and alloys, and may be prepared as foils, disks or composites (through the electroplating, sputtering, sedimenting, or pressing of alloys and elements onto supporting metal substrates (target backing) such as gold, silver, tantalum, titanium, rhodium or niobium).7-10 The specific design selected depends on factors such as substrate bond, heat transfer efficiency, ease of product isolation from the target material after irradiation, ease of target material recovery for enrichedmaterial targets, product sensitivity to impurities and nuclear cross-section data.8 An ideal target should be stable, allow a high rate of heat transfer, and possess favorable melting properties⁶ since proton-induced irradiation generates significant amounts of heat in a small target area. When heat transfer and melting point are not suitable, innovations such as an oblique target arrangement as well as target alloying practices have been implemented to pacify these limitations. The separation chemistry employed should be fast (i.e. less than one half-life of the product radionuclide) and efficient at separating the product from both the target material and co-produced impurities.11 Commonly used separation techniques include are ion exchange chromatography, solid phase extraction (SPE) and thermochromatographic dry distillation, the schematics for which can be seen in Fig. 2, Fig. 3 and Fig. 4 respectively.

The radioisotopes covered in this review (see Table 1) can be produced on solid targets using small-to-medium sized, protonaccelerating cyclotrons with a maximum particle acceleration energy of 24 MeV. Production using this class of cyclotron was selected since these machines are the most prevalent in medical and research institutions. While the list of radioisotopes reviewed is a comprehensive one, the authors would like to highlight other PET radioisotopes such as \$^{110m}In^{12,13}\$, \$^{152}Tb,^{13,14}\$ 51 Mn, 15,16 62 Cu $^{16-18}$ and 132 La 19,20 which are also available for production on the aforementioned cyclotrons, but were excluded from this review due to limitations. This review briefly discusses the biomedical application of each radionuclide while focusing mainly on the specifics of its production and purification procedures. Several recent reviews can provide more

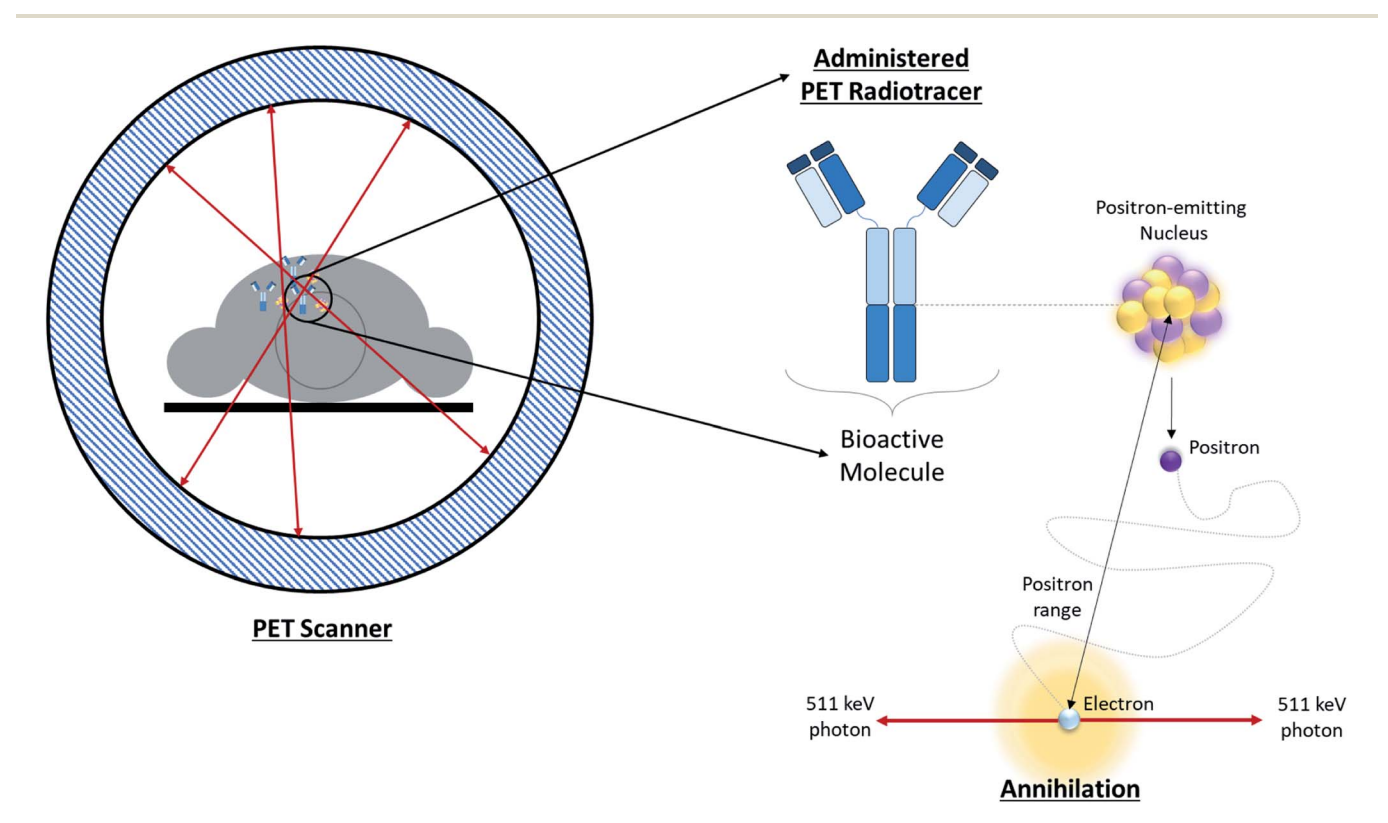


Fig. 1 Overview of PET. Schematic depicting positron annihilation in a patient undergoing a PET scan.

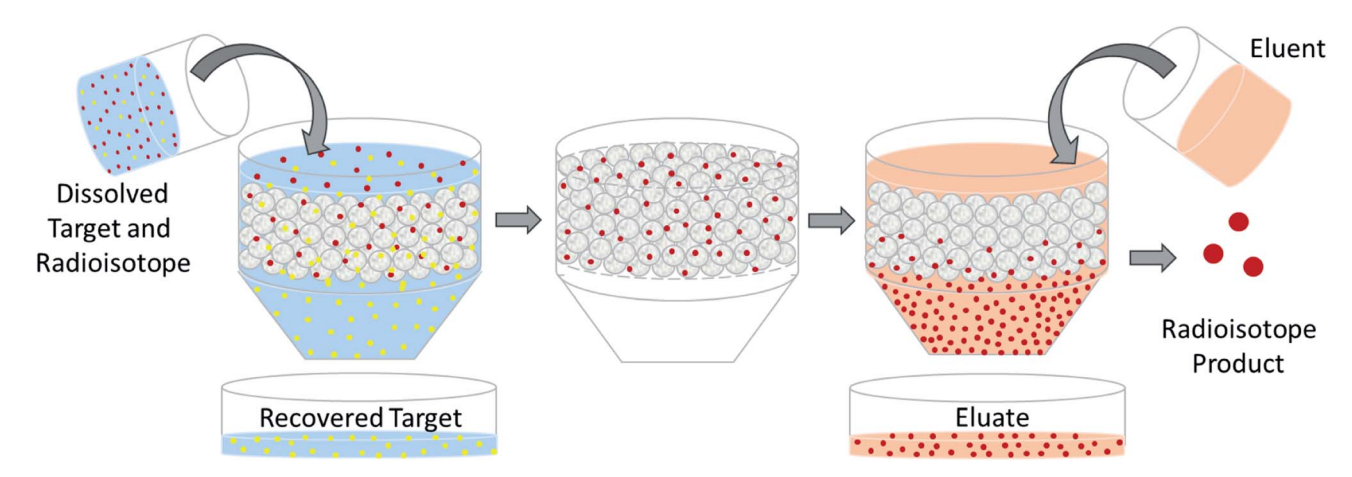


Fig. 2 Ion exchange chromatography. Schematic depicting the separation of dissolved PET radioisotopes from dissolved, unreacted target material after passage through an ion exchange column. The resin retains the PET radioisotope, and an eluent is used for its elution.

details on the applications of established and emerging PET radionuclides discussed herein ref. 21-23. A summary of the major nuclear and production properties of each radioisotope is provided in Table 1 for convenience. The nuclear information presented in this review was retrieved from the National Nuclear Data Center website by Brookhaven National Laboratory (https://www.bnl.gov).

List of PET radioisotopes

Halogens

Bromine: 75Br, 76Br

Applications. Since the early days of nuclear medicine, several bromine isotopes have been considered for therapy (auger emitting ⁷⁷Br), SPECT (^{80m}Br), and for PET imaging (⁷⁵Br and

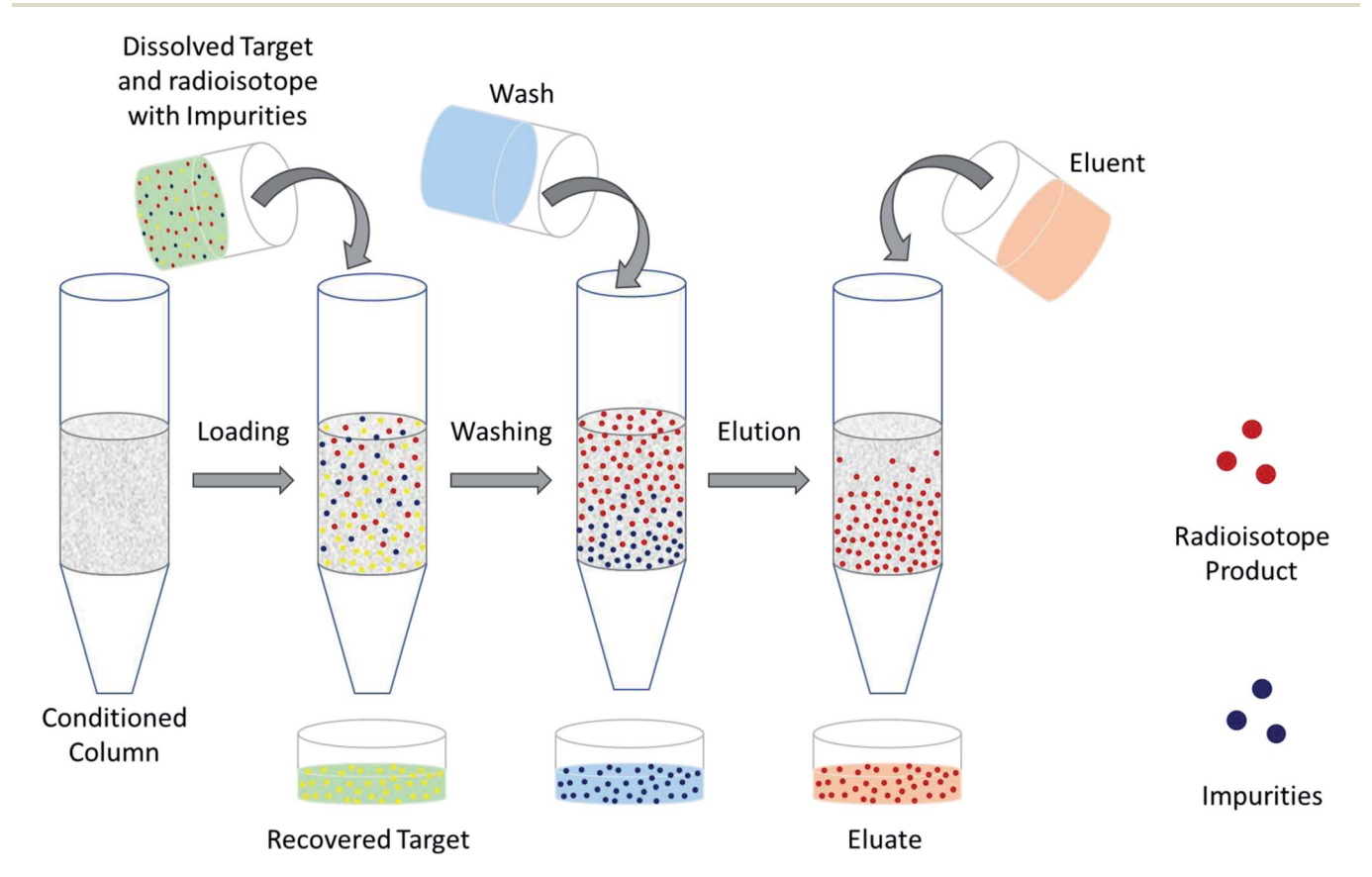


Fig. 3 Solid phase extraction. Schematic depicting the separation of dissolved PET radioisotopes from dissolved, unreacted target material after passage through a solid phase extraction column. The column retains the PET radioisotope and any impurities. Impurities are washed-off before elution is performed to obtain the PET radioisotope.

Review

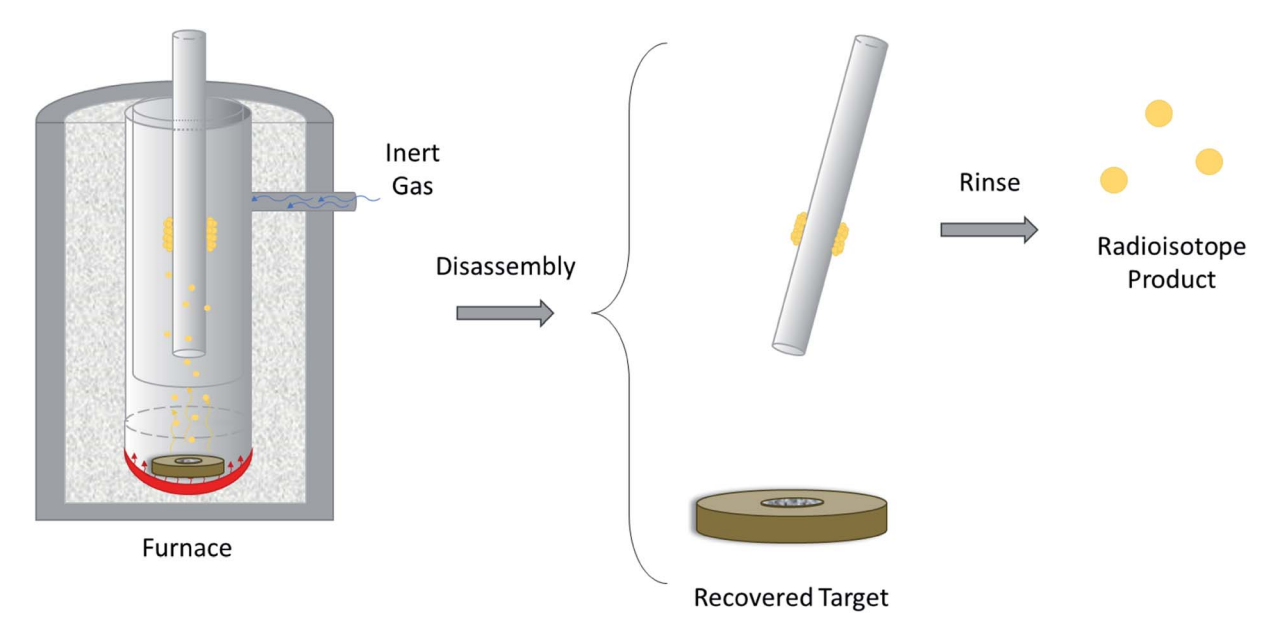


Fig. 4 Thermochromatographic dry distillation. Schematic depicting the separation of volatile PET radioisotopes from non-volatile target material after heating is performed in a furnace. The PET radioisotope condenses on a removable, cooler surface within the furnace. The radioisotope is removed from the surface using a rinse.

⁷⁶Br). With intermediary physicochemical properties between fluorine and iodine, radiobromines allow for fine-tuning molecular mass, volume, polarizability, and lipophilicity as alternatives to fluorine-18 (18 F; $t_{1/2}$: 109.8 min, 100% β^+) or radioiodines (see next section). Of the two positron emitting bromine isotopes, 75 Br ($t_{1/2}$: 96.7 min, 75% β^+ , 25% EC), has the more favorable characteristics for PET applications with a larger yield of lower energy positrons and a lower number of other gamma-generating decay modes. While the long half-life daughter 75 Se ($t_{1/2}$: 119.8 d, 100.0% EC) warrants careful dose estimation, several 75Br-labeled agents have undergone preclinical and clinical studies including cardiac fatty acid metabolism,24 neuroreceptor mapping,25-28 and glucose analogues.29

The other positron-emitting isotope is 76 Br ($t_{1/2}$: 16.2 h, 55% β^+ , 45% EC). It has seen wider adoption primarily because it decays to stable ⁷⁶Se^{1,30,31} and possesses a half-life well matched to protein pharmacokinetics as illustrated through ⁷⁶Br-labeled antibodies and their fragments for preclinical tumor imaging.1 Beyond antibody radiolabeling, there are examples of ⁷⁶Brlabeled neuroimaging tracers,32-34 peptides,35 reporter gene studies,36 and agents for studying sympathetic innervation.37 Despite this there are limitations to using ⁷⁶Br-labelled tracers for PET imaging applications. Similar to radioiodine, it is prone to dehalogenation in vivo where it generally remains in blood circulation and slowly accumulates in the gastric mucosa. 38 The high levels of blood retention negatively affects image quality, particularly in blood rich organs (i.e. the heart and lungs) hours after the tracer has been administered.1,38 Furthermore, bromide has a long biological half-life in human plasma (about 10 days) which makes elimination of labile [76Br]Br postimaging problematic.39 These concerns will surely be addressed as new 76Br-labelled tracers are developed, given an

expanded role of this isotope with new $\beta^+ \gamma$ coincidence PET methodologies. 40,41 A recent review of the chemistry and applications of radiobromines⁴² provides more insight into their applications.

Production. The primary nuclear reaction used to produce ⁷⁵Br on solid-target medical cyclotrons is the ⁷⁶Se(p,2n)⁷⁵Br nuclear reaction.30,43-46 Although enriched elemental selenium has been used to produce solid targets for proton bombardment,30,44-46 its low melting point and low thermal conductivity necessitates current restrictions to maintain target integrity during bombardment. Alloyed selenides such as NiSe, Ag₂Se, CuAgSe, Cu₂Se and PbSe^{30,44,47} have been developed as suitable alternatives which permit irradiation at higher currents, significantly increasing yields. One drawback of selenium alloy targets is poor adherence to heat-conducting target backings.44 The beam energy used for the production of ⁷⁵Br ranges from 24 to 21.5 MeV. 43,44 For this energy range, the theoretical 75 Br yields (assuming ⁷⁶Se-enriched targets), ranged from 1184 to 1480 MBq $(\mu A h)^{-1}$ (i.e. 32-40 mCi $(\mu A h)^{-1}$), 44 although production at higher energies (i.e. 28 to 22 MeV) provided yields up to three times greater.30 The major impurity produced was 76Br43-45 although trace amounts of 72 As ($t_{1/2}$: 26.0 h, 87.8% β^+ , 12.2% EC), ⁷³As ($t_{1/2}$: 80.3 d, 100.0% EC), ⁷⁵Se ($t_{1/2}$: 119.8 d, 100.0% EC) and ⁷⁷Br ($t_{1/2}$: 57.0 h, 0.7% β^+ , 99.3% EC) have been reported.⁴⁴

There are several reactions that can be used to produce ⁷⁶Br, however few can be carried out using lower-energy medical cyclotrons.46 Nevertheless, a feasible production route is the ⁷⁶Se(p,n)⁷⁶Br nuclear reaction, which occurs in the 16 to 8 MeV beam energy range. 48 Like 75Br, the target was composed of an enriched selenium alloy, specifically Cu₂Se^{48,49} or NiSe.⁴⁷ Bombarding a Cu₂Se target with beam energies ranging from 16 to 8 MeV, the yield of ⁷⁶Br ranged from 65 to 70 MBq (μ A h)⁻¹ (*i.e.* 1.8 to 2.1 mCi $(\mu A h)^{-1}$) at end of bombardment (EOB).⁴⁸ The

Table 1 Properties of emerging and commonly used PET radionuclides

		Nuclear properties					Production conditions			
Element	Isotope		Mode of decay (%)		β ⁺ endpoint energy, keV (%)	Principal γ energies, keV (Abs. %)	Major nuclear reactions	Beam energy, MeV	Target	Max. reported yield, MBq (μA h) ⁻¹
Arsenic (As)	72	26.0 h	β ⁺ (87.8) EC (12.2)		2500 (64.2) 3334 (16.3)	511 (176.4), 630 (8.1), 834 (81.0), 1464 (1.13)	⁷² Ge(p,n) ⁷² As	18-8	Natural or enriched GeO ₂ on Cu or Nb, Ge foil	90
Bromine (Br)	75	96.7 min	β^{+} (75.0) EC (25.0)	-	1753 (53.0), 1612 (4.9), 2040 (4.0)	511 (149.1),141 (6.6), 287 (88.0), 428 (4.4)	⁷⁶ Se(p,2n) ⁷⁵ Br	24-21.5	Enriched Se, enriched selenides (<i>i.e.</i> Ag ₂ Se, CuAgSe, Cu2Se, PbSe)	1480
	76	16.2 h	β ⁺ (55.0) EC (45.0)	1532, 375, 1800	3382 (25.8), 871 (6.3), 3941 (6.0)	511 (109), 559 (74.0), 657 (15.9), 1854 (147)	⁷⁶ Se(p,n) ⁷⁶ Br	16-8	Enriched Se, enriched selenides (<i>i.e.</i> Cu ₂ Se)	70
Copper (Cu)	60	23.7 min	β ⁺ (93.0) EC (7.0)	872, 1325, 840	1982 (49.0), 2947 (15.0), 1912 (11.6)	511 (185.0), 826 (21.7), 1333 (88.0), 1792 (45.4)	⁶⁰ Ni(p,n) ⁶⁰ Cu	14.7	Natural or enriched Ni on Au	2146
	61	3.3 h	β ⁺ (61.0)	524, 399	1216 (51.0), 933 (5.8)	511 (123.0), 67 (4.2), 282 (12.2),	⁶¹ Ni(p,n) ⁶¹ Cu	14.7-9	Enriched Ni on Au	281
			EC (39.0)			656 (10.8)	64 Zn(p, α) 61 Cu	17.6- 11.7	Natural or enriched Zn	13
	64	12.7 h	β ⁺ (17.6) β ⁻ (38.5) EC (43.9)	278	653 (17.6)	511 (35.2), 1346 (0.5)	⁶⁴ Ni(p,n) ⁶⁴ Cu	15-10	Enriched Ni on Au or Rh	5883
Cobalt (Co)	55	17.5 h	β ⁺ (76.0) EC (24.0)		1499 (46.0), 1021 (25.6)	511 (152.0), 477 (20.2), 931 (75.0), 1409 (16.9)	$^{56}{ m Fe}({ m p,2n})^{55}{ m Co}$ $^{58}{ m Ni}({ m p,}\alpha)^{55}{ m Co}$	23.5-16 16-15	Enriched Fe Enriched Ni, enriched Ni on Ag or Au	236
Gallium (Ga)	66	9.5 h	β ⁺ (57.0) EC (43.0)		4153 (51.0), 924 (3.7)	511 (114.0), 834 (5.9), 1039 (37.0), 2752 (22.7)	⁶⁶ Zn(p,n) ⁶⁶ Ga	15-6	Natural or enriched Zn on Au or Ag	700
	68	67.7 min	β ⁺ (88.9) EC (11.1)		1899 (87.7), 822 (1.2)	511 (177.8), 1077 (3.2), 1261 (0.1), 1883 (0.1)	⁶⁸ Zn(p,n) ⁶⁸ Ga	14-11	Enriched Zn, enriched Zn on Al, Au or Ag	1380
Iodine(1)	124	4.2 d	β^{+} (22.7) EC (77.3)		1535 (11.7), 2138 (10.7)	511 (45.0), 603 (62.9), 723 (10.4), 1691 (11.2)	^{124,125} Te(p,xn) ¹²⁴ I	22-5	Natural or enriched Te, natural or enriched TeO ₂	111
Manganese (Mn)	52g	5.6 d	β ⁺ (29.4) EC (70.6)	242	575 (29.4)	511 (58.8), 744 (90.0), 936 (94.5), 1434 (100.0)	⁵² Cr(p,n) ^{52g} Mn	20-10	Natural Cr, natural Cr on Cu or Ag	9.6
Niobium (Nb)	90	14.6 h	β ⁺ (53.0) EC (47.0)		1500 (51.0), 1641 (2.0)	511 (102.0), 142 (66.8), 1129 (92.7), 2319 (82.0)	^{90,91} Zr(p,xn) ⁹⁰ Nb	19–7	Natural Zr, enriched ZrO ₂ on Cu	596
Scandium (Sc)	44g	4.0 h	β ⁺ (94.3) EC (5.7)	632	1474 (94.3)	511 (188.5), 1157 (99.9), 1499 (0.9)	⁴⁴ Ca(p,n) ^{44g,m} Sc	18-6	Natural or enriched Ca, enriched CaO ₃	50
Technetium (Tc)	94m	52 min	β ⁺ (70.2) EC (29.8)		2439 (67.6), 1446 (0.9), 917 (0.9)	511 (140.3), 871 (94.2)	⁹⁴ Mo(p,n) ^{94m} Tc	13-6	Natural Mo, enriched MoO ₃	111
Titanium (Ti)	45		β ⁺ (84.8) EC (15.2)	439	1040 (84.8)	511 (169.6), 720 (0.2), 1408 (0.1)	45 Sc(p,n) 45 Ti	16-8	Natural Sc	422
Yttrium (Y)	86g		β ⁺ (31.9) EC (68.2)		1221 (11.9), 1545 (5.6), 1988 (3.6)	511 (64.0), 628 (32.6), 1077 (82.5), 1153 (30.5)	⁸⁶ Sr(p,n) ^{86g} Y	15.1–11	Enriched SrCO ₃ or SrO	166
Zinc (Zn)	63	38.5 min	β ⁺ (92.7) EC (7.3)	1042, 733, 600	2345 (80.3), 1675 (7.0), 1382 (4.9)	511 (185.5), 670 (8.2), 962 (6.5), 1412 (0.8)	⁶³ Cu(p,n) ⁶³ Zn	16-6	Natural or enriched Cu	2470
Zirconium (Zr)	89	78.4 h	β ⁺ (22.7) EC (77.3)	396	902 (22.7)	511 (45.5), 909 (99.0), 1713 (0.7), 1745 (0.1)	⁸⁹ Y(p,n) ⁸⁹ Zr	14-9	Natural Y, natural Y_2O_3 on Cu	58

Table 2 Production and purification parameters for ⁷⁵Br and ⁷⁶Br

Radioisotope	⁷⁵ Br, ⁷⁶ Br
Target material	Elemental selenium, selenides
	(NiSe, Ag ₂ Se, CuAgSe, Cu ₂ Se, PbSe)
Product purity	_
Major impurities	⁷⁶ Br, ⁷² As, ⁷³ As, ⁷⁵ Se, ⁷⁷ Br
Separation method	Thermochromatographic dry distillation
•	(300–1100 °C in Ar; water or ethanol for
	precipitate dissolution; NaOH trap)
Product separation yield	65-75%
Target recovery yield	(100 - x)%, where 'x' is no. of times reused

primary impurity produced for this production route was ⁷⁷Br (2%). ^{30,46}

Product purification and target recovery. The primary method used to isolate bromine from irradiated selenium was thermochromatographic dry distillation. 30,43,44,46,48 This procedure required heating the selenide targets in an enclosed, oxygenfree apparatus such as a furnace or dedicated distillation vessel. The distillation temperature depended on the type of target being processed, with 300 °C being ideal for distillation of bromine from elemental selenium targets^{43,44} and temperatures ranging from 1090 to 1100 °C being ideal for the selenide targets. 30,48 To ensure an oxygen-free environment, an inert gas such as argon was continuously passed through the system. In addition to reducing oxygen exposure, the argon gas mobilizes vaporized bromine and selenium gases generated from the distillation out of the furnace and into a cold trap for collection. The vaporized selenium was the first to condense along the walls of the tubing at temperatures between 120 and 215 °C,44 while the bromine began to condense closer to room temperature. Any uncondensed bromine can be collected by bubbling the gas stream through water44 or a dilute NaOH solution.48 The condensed bromine can be removed by washing with pure water or absolute ethanol.30,44 Once cooled, the heated targets can be recycled and repeatedly irradiated, typically up to 20 times with <1% target material loss per run. 30,48 The product separation yield for the process ranged from 65-75%.48

Summary. Table 2 below summarizes key production and purification parameters for $^{75}{\rm Br}$ and $^{76}{\rm Br}$ not hitherto mentioned in Table 1.

Iodine: 124I

Applications. Apart from 99m Tc, radioiodines are the most commonly used radionuclides in nuclear medicine. Complementary to the near ideal SPECT isotope 123 I ($t_{1/2}$: 13.2 h, 100.0% EC), the positron emitting 124 I ($t_{1/2}$: 4.2 d, 22.7% β^+ , 77.3% EC) has been used extensively in immunoPET imaging and other protein-based PET applications due to its well-understood radiochemistry and long half-life. 1,50 Thus far, 124 I has been used for cancer diagnosis, monitoring and treatment planning, as well as mechanistic, and pharmacokinetic studies. $^{51-54}$ Beyond antibodies, 124 I labelled peptides and small molecules targeting neurotransmitters systems, tumor hypoxia, prostate specific membrane antigen (PSMA), and neuroinflammation have also been investigated in humans. $^{55-57}$ However, the use of

¹²⁴I is not without its limitations, not the least of which is its comparatively low positron yield at a high end-point energy. This results in low spatial resolution58 which may be addressed through hybrid imaging with PET/MR instruments possessing strong magnetic fields. 59 Another drawback is the large number of gammas released from electron capture, increasing patient radiation dose, and further limiting image resolution. These can be corrected for with special software^{1,3} and may be turned into an advantage using the aforementioned β^+/γ coincidence tomography. 41 To avoid high doses to the thyroid gland from the high energy positron and gammas, ideally the attachment of ¹²⁴I to biomolecules is kinetically inert. ⁶⁰ Readers are referred to recent reviews on the radiochemistry and application of radioiodines for more information.23,42 Taking advantage of increased interest in theranostic radiopharmaceuticals, 124I may see a surge in upcoming years as a companion to 131 I ($t_{1/2}$: 8.02 d, β⁻: 971 keV) or used for therapy itself (70% absorbed dose of 131 I.61

Production. While 124I can be produced through a number of different nuclear reaction pathways, however the most feasible production via low-energy proton cyclotron is through the 124,125 Te(p,xn) 124 I nuclear reactions. The radioisotope can be produced through the irradiation of natural tellurium (isotopic composition: 0.09% ¹²⁰Te, 2.55% ¹²²Te, 0.89% ¹²³Te, 4.74% ¹²⁴Te, 7.07% ¹²⁵Te, 18.84% ¹²⁶Te, 31.74% ¹²⁸Te, 34.08% ¹³⁰Te) metalloid targets, >98% enriched 124,125 Te metalloid targets, and enriched tellurium oxides electro-deposited or melted onto platinum or tantalum substrates. The optimum beam energy range used for irradiation can range from 14 to 5 MeV for 124Tebased targets, and 22 to 4 MeV for 125Te-based targets. The primary impurities produced during bombardment using 124Tebased targets were 123 I ($t_{1/2}$: 13.2 h, 100.0% EC), 125 I ($t_{1/2}$: 59.4 d, 100.0% EC), 126 I ($t_{1/2}$: 12.9 d, 1.0% β^+ , 47.3% β^- , 51.7% EC) and 130 I ($t_{1/2}$: 12.4 h, 100.0% β^{-}), while the primary impurities for ¹²⁵Te-based targets are ¹²³I and ¹²⁵I. ^{9,46,54,62,63} For the ¹²⁴Te(p,n)¹²⁴I nuclear reaction within the 14 to 7 MeV energy range, reported yields ranged from 5 to 21 MBq (μ A h)⁻¹ (i.e. 0.1 to 0.6 mCi (μ A h)⁻¹) with major impurities equaling less than 1%. For the ¹²⁵Te(p,2n)¹²⁴I nuclear reaction within the 22 to 4 MeV energy range, reported yields ranged from 43 to 111 MBq $(\mu A h)^{-1}$ (i.e. 1.2 to 3.0 mCi $(\mu A h)^{-1}$) with impurities comprising as much as 13% of the final product.54,62-64

Product purification and target recovery. The preferred method for separating the radioiodine from the post-bombarded tellurium target material is via dry (thermochromatographic) distillation, 46,54,63 which is facilitated by the favorable melting and solidification properties of TeO₂. Conventional dry distillation was carried out using a ventilated quartz tube where the irradiated TeO₂ was heated to temperatures between 670 to 820 °C for periods ranging from 5 to 20 min in carrier gases of either air, argon, helium, or oxygen. This approach aimed to extract as much of the iodine product using a NaOH trap, however, any prematurely condensed iodine can be removed via dissolution using a weak buffer solution. To minimize tellurium evaporation, Al₂O₃/quartz wool was integrated into the distillation setup. The separation efficiency for the dry distillation stage ranged from 80% to 95%. Wet chemistry methods were

Review RSC Advances

also used to chemically isolate iodine from the tellurium targets, but these methods were less preferred due to product dilution in the final solution. The process was carried out in two stages, with the first being a target dissolution stage using an oxidizing alkali, and the second a reduction stage facilitated by the addition of aluminum powder.⁹

After the iodine has been extracted, the spent tellurium targets can be recycled. Metallic tellurium targets can be dissolved in a mixture of hydrogen peroxide and hydrochloric acid, and the resulting solution can subsequently be reduced using either hydrogen bromide or a mixture of hydrazine and sodium sulfite. Reduction *via* the former recovered tellurium in the form of tellurite, while the latter facilitated the recovery of metallic tellurium.⁹ For tellurium oxide targets, a multistage process involving vacuum distillation, acid dissolution and chemical precipitation was used to recover metallic tellurium.⁹ In general, the recovery yields for tellurium-based targets range from 60 to 90%.⁵⁴ However, despite the innovations in tellurium recovery, ¹²⁴I production is still negatively affected by high target material costs.⁶²

Summary. Table 3 summarizes key production and purification parameters for ¹²⁴I not previously mentioned in Table 1.

Transition metals

Copper: 60Cu, 61Cu and 64Cu

Applications. Copper has many positron-producing radionuclides (*i.e.* 60 Cu ($t_{1/2}$: 23.7 min, 93.0% β^+ , 7.0% EC), 61 Cu ($t_{1/2}$: 3.3 h, 61.0% β^+ , 39.0% EC) and 64 Cu ($t_{1/2}$: 12.7 h, 17.6% β^+ , 38.5% β -, 43.9% EC)) that are finding use in PET applications primarily due to their well-established coordination chemistry. 10 Although less frequently utilized, 60 Cu and 61 Cu have been used to label various bioactive molecules for hypoxia and blood flow studies. 17,21,65

The most commonly used copper radioisotope is ⁶⁴Cu, with the first-in-human use as [⁶⁴Cu]ASTM for tumor hypoxia. ⁶⁶ There are several characteristics that make ⁶⁴Cu well suited for PET imaging. Besides its well elucidated chemistry, its favorable half-life allows it to be used for radiolabeling various targeting vectors like peptides, antibodies, and nanoparticles. ^{1,10} Additionally, the positron energy for ⁶⁴Cu (mean: 278 keV, max: 653 keV) is comparable to ¹⁸F (mean: 250 keV, max: 634 keV), leading to similar positron range and excellent spatial resolution. ⁶⁷ With respect to use in immunoPET, there exists some dissonance between radiolabeling conditions and antibody stability. Moreover, some ⁶⁴Cu radiotracers were found to be

susceptible to metabolism in the liver, which permits transchelation of the radioisotope with other copper-binding proteins such as Cu/Zn superoxide dismutase (Cu/Zn SOD) in the liver and metallothionein in the blood. ^{1,3,68} These limitations may be overcome with improved chelator technology. ^{69,70} Lastly, it warrants mentioning the potential theranostic pairing with ⁶⁷Cu ($t_{1/2}$: 2.58 d, β ⁻: 100%, avg. E_{β} -: 141 keV) which makes it ideal for radioimmunotherapy monitoring. ⁷¹

Production. As 60 Cu is typically produced *via* the 60 Ni(p,n) 60 Cu nuclear reaction, occurring with natural nickel (isotopic composition: 68.08% 58 Ni, 26.22% 60 Ni, 1.14% 61 Ni, 3.63% 62 Ni, 0.93% 64 Ni) and enriched 60 Ni targets when bombarded with a beam energy of 14.7 MeV. 65 For the 14.7 MeV bombardment of >99% enriched 60 Ni electroplated on a gold target backing, the yield at EOB was 2146 MBq (μA h) $^{-1}$ (*i.e.* 58 mCi (μA h) $^{-1}$) with the primary impurities produced to include 61 Cu ($t_{1/2}$: 3.3 h, 61.0% β $^{+}$, 39.0% EC) (0.05%) and 57 Co ($t_{1/2}$: 271.7 d, 100.0% EC) (0.025%). 65 When bombardment was carried out using natural nickel targets for similar conditions in the same study, EOB yields of 291 MBq (μA h) $^{-1}$ (*i.e.* 7.9 mCi (μA h) $^{-1}$) and 385 MBq (μA h) $^{-1}$ (*i.e.* 10.4 mCi (μA h) $^{-1}$) were reported along with the presence of 55 Co ($t_{1/2}$: 17.5 h, 76.0% β $^{+}$, 24.0% EC) (0.65%) and 61 Cu (0.60%) as the major impurities. 65

Both the ${}^{61}\text{Ni}(p,n){}^{61}\text{Cu}{}^{65,72}$ and ${}^{64}\text{Zn}(p,\alpha){}^{61}\text{Cu}{}^{17,72}$ nuclear reactions have been reported for the production of 61Cu. Production via ⁶¹Ni(p,n)⁶¹Cu required proton optimum beam energies ranging from 14.7 to 9 MeV and enriched ⁶¹Ni targets. For the 14.7 MeV bombardment of >99% enriched 61Ni electroplated onto a gold target substrate with a thickness of 118 µm and diameter of 5 mm, the ⁶¹Cu yield at EOB was 281 MBq (μA h)⁻¹ (i.e. 7.6 mCi (μ A h)⁻¹) while the primary impurity produced was 58 Co ($t_{1/2}$: 70.9 d, 14.9% β^+ , 85.1% EC) (0.04%). 65 In the same study, 60Ni(d,n)61Cu reactions were investigated but produced lower yields at higher per bombardment costs. Alternatively, 61 Cu can be produced using the 64 Zn(p, α) 61 Cu nuclear reaction. The reaction has been investigated with natural zinc (isotopic composition: 49.17% ⁶⁴Zn, 27.73% ⁶⁶Zn, 4.04% ⁶⁷Zn, 18.45% ⁶⁸Zn, 0.61% ⁷⁰Zn) foils and enriched ⁶⁴Zn electroplated on to gold, silver or aluminum substrates with beam energies ranging from 17.6 to 11.7 MeV (maximum production occurs circa 14.5 MeV).17 When >99% enriched 64Zn was bombarded with 14.5 MeV protons, the yield of ⁶¹Cu was 13 MBq $(\mu A h)^{-1}$ (i.e. 0.4 mCi $(\mu A h)^{-1}$) with a purity exceeding 95%.17 Despite having completed similar experiments using natural zinc foil targets in the same study, the results were too

Table 3 Production and purification parameters for ¹²⁴I

Radioisotope	$^{124}\mathrm{I}$
Target material	Natural and enriched tellurium, enriched tellurium oxide
Product purity	87->99%
Major impurities	123 I, 125 I, 126 I, 130 I
Primary separation method	Thermochromatographic dry distillation
	(670–820 °C in air, Ar, He or O ₂ ; weak buffer for precipitated dissolution; NaOH trap)
Product separation yield	80-95%
Target recovery yield	60–90%

RSC Advances Review

variable to draw valid conclusions. The primary impurities produced during the bombardment of zinc targets were 66 Ga ($t_{1/}$ ₂: 9.5 h, 57.0% β^+ , 43.0% EC), ⁶⁷Ga ($t_{1/2}$: 3.3 d, 100.0% EC) and ⁶⁸Ga ($t_{1/2}$: 67.7 min, 88.9% β⁺, 11.1% EC). ¹⁷ Based on the data generated, ⁶¹Cu production from the bombardment of nickel was found to be more efficient than production using zinc. However, the former production route can be expensive due to the high cost associated with enriched ⁶¹Ni. Since enriched ⁶⁴Zn is significantly cheaper than enriched ⁶¹Ni, the production of ⁶¹Cu from zinc targets has found some consideration as an alternative route.17

⁶⁴Cu is primarily produced *via* the ⁶⁴Ni(p,n)⁶⁴Cu nuclear reaction. 9,62 The solid target used for the production is typically enriched ⁶⁴Ni that has been electroplated onto a gold^{62,73-77} or rhodium¹⁰ target backing substrate. Although the threshold for the reaction is 2.5 MeV, production of ⁶⁴Cu has been reported for beam energies ranging from 15 to 10 MeV since this range offers the highest yields.⁶² Numerous yields for the production of ⁶⁴Cu have been reported in the literature. McCarthy et al. ⁷⁶ reported yields ranging from 85 to 185 MBq (μ A h)⁻¹ (i.e. 2.3 to 5 mCi (μA h)⁻¹) when gold substrates electroplated with >95% ⁶⁴Ni (thicknesses ranging from 132 to 311 μm) were bombarded with a 15.5 MeV proton beam, while McCarthy et al.65 reported yields of 296 MBq $(\mu A h)^{-1}$ (i.e. 8 mCi $(\mu A h)^{-1}$) for greater purity targets of similar design (i.e. >99% 64Ni electroplated onto a gold substrate with a thickness of 215 µm and diameter of 5-6 mm) irradiated at 14.7 MeV. Obata et al.77 reported yields ranging from 22 to >111 MBq (μ A h)⁻¹ (i.e. 0.6 to >3 mCi (μ A h)⁻¹) when they bombarded gold substrates that were electroplated with 94.8% ⁶⁴Ni with a 12 MeV proton beam. More recently, a saturation yield of 5883 MBq (μ A h)⁻¹ (i.e. 159 mCi $(\mu A h)^{-1}$) has been reported by Avila-Rodriguez et al. (2007) when they bombarded gold substrates electroplated with >95% enriched 64Ni with an 11.4 MeV proton beam. The primary impurity produced for this reaction is 55 Co ($t_{1/2}$: 17.5 h, 76.0% β^+ , 24.0% EC) (0.012%).65 However, other relevant impurities include ⁵⁷Ni ($t_{1/2}$: 35.6 h, 43.6% β^+ , 56.4% EC), ⁵⁶Co ($t_{1/2}$: 77.2 d, 19.7% β^+ , 80.3% EC), ⁵⁷Co ($t_{1/2}$: 271.7 d, 100.0% EC) and ⁵⁸Co ($t_{1/2}$: 70.9 d, 14.9% β⁺, 85.1% EC).⁷³

Product purification and target recovery. Isolation of the copper product from the target material begins with target dissolution in strong acid (i.e. 6 M HNO₃ or 6 N HCl at temperatures ranging from 90 to 100 °C (Jeffery et al. 2012). The acidic solution is passed through an anion exchange column filled with AG1-X8 resin which retains the copper product along with the nickel target material and any cobalt impurities present. The nickel target material is eluted first using 6 N HCl^{75,76} for HCl-dissolved targets, or 0.2 M HCl in 96% methanol⁷⁴ for HNO₃-dissolved targets. The cobalt impurity fraction retained by the column can be eluted with 4 M HCl⁷⁵ for HCl-dissolved targets, or 0.3 M HCl in 72% ethanol⁷⁴ for HNO₃-dissolved targets. Finally, the copper product can be eluted using dilute acid (i.e. 0.1-0.5 M) or distilled water^{75,76} for HCl-dissolved targets, or 0.3 M HCl in 40% ethanol74 for HNO3-dissolved targets. Separation yields exceeding 95% have been reported for the process.75

Implementation of a dedicated recycling scheme for 60Ni recovery is not typical due to its low material cost,65 which stems

from the large natural abundance of the isotope. However, recycling of enriched ⁶⁴Ni is necessary to keep production costs down. Several methods have been developed for 64Ni recovery. The method described by Obata et al.77 made use of two heating stages conducted in series. In the first heating stage, the solution containing the eluted nickel was evaporated to dryness at 150 °C before it was rehydrated with distilled water. In the second heating stage, the rehydrated solution was heated at 900 °C for 24 h. This resulted in the formation of ⁶⁴NiO which was then used for the preparation of future targets. The minimum recycling efficiency for this process was 94%. A second method was discussed by McCarthy et al.,76 and required several evaporation and acid dissolution steps be carried out in series. The first two acid dissolution steps were performed with HNO₃ and the final acid dissolution step was performed with H₂SO₄. After H₂SO₄ dissolution, the solution was diluted and the pH was adjusted to 9 with the addition of concentrated NH₄OH. The solution was available for electroplating after the addition of ammonium sulfate and a final dilution with deionized water. The overall efficiency of this recovery process exceeded 90%.

For the case of 61Cu production from zinc targets, Rowshanfarzad et al.72 and Asad et al.17 outlined a method which made use of multiple column separation stages in series. The zinc portion of the targets were dissolved in 10 M HCl at room temperature before passing through a cation exchange column filled with AG 50W-X8 resin (200-400 mesh). The column retained the copper product, the gallium impurities, and the unreacted zinc target material. The copper product and zinc target materials were eluted with 10 M HCl and the eluant was passed through an AG 1-X8 anion exchange column (200-400 mesh). Both the copper product and zinc target material were retained, and the copper product was selectively eluted with 2 M HCl. In order to recycle the zinc target material (as in the case of enriched targets), the column can be eluted with 0.5 M HCl.¹⁷ This solution was then evaporated to dryness before 6 M H₂SO₄ was added to digest any resin residues from the prior chromatography stages. The evaporation/digestion stage was repeated before the recovered zinc was finally reconstituted as an electroplating solution. The overall yield for the 64Zn recovery process was about 90%.17

Summary. Table 4 summarizes key production and purification parameters for ⁶⁰Cu, ⁶¹Cu and ⁶⁴Cu not mentioned in Table 1.

Cobalt: 55Co

Applications. Cobalt is a human micronutrient and component of the essential vitamin B₁₂ (cobalamin). As a potential competitor radionuclide to 64 Cu, 55 Co ($t_{1/2}$: 17.5 h, 76.0% β^+ , 24.0% EC) has been shown to mimic calcium intake in infarcted brain tissue. This property makes it useful in the imaging of recent cerebral brain damage resulting from cerebral tumors, stroke and other brain injuries.78-81 Recent reports have demonstrated high resolution PET images obtained with peptide and affibody chelates of 55Co.82,83 Ionic 55Co species are residualizing radiotracers. Significant amounts of 55Co can accumulate in organs such as the bladder, liver and kidney84 with the majority eliminated or decayed three days postinjection. 55Co has also shown great promise in the field of

immunoPET imaging and has been used to label an anti-EGFR affibody⁸² as well as several peptides. ^{83,85} Unfortunately, widespread clinical use of this isotope may be hampered as ⁵⁵Co decays into ⁵⁵Fe ($t_{1/2}$: 2.73 years) while releasing large amounts of high energy gamma rays from electron capture in the process. ¹ Nonetheless, it remains a valuable tool for preclinical PET investigations.

Production. There are two major nuclear reactions available to produce ⁵⁵Co on small medical cyclotrons by utilizing either the 56 Fe $(p,2n)^{55}$ Co^{81,86,87} or the 58 Ni $(p,\alpha)^{55}$ Co.^{81,88,89} Production *via* ⁵⁶Fe(p,2n)⁵⁵Co involved irradiating ⁵⁶Fe-enriched iron foils⁸⁷ with a minimum proton beam energy of about 16 MeV,86,87 although the reaction peaks at an energy near 23.5 MeV.87 However, this production route was undesirable since significant amounts of the chemically-inseparable 56 Co ($t_{1/2}$: 77.2 d, 19.7% β⁺, 80.3% EC) impurity was also co-produced.⁸¹ The ⁵⁸Ni(p,α)⁵⁵Co production route can be carried out through the bombardment of natural nickel (isotopic composition: 68.08% ⁵⁸Ni, 26.22% ⁶⁰Ni, 1.14% ⁶¹Ni, 3.63% ⁶²Ni, 0.93% ⁶⁴Ni) foils⁸⁹ or enriched ⁵⁸Ni-electroplated onto silver⁸⁸ or gold⁸¹ disk substrates. Irradiations have been carried out using proton beams with energies of about 16 MeV (ref. 88 and 90) to 15 MeV.81 The primary impurities produced during irradiation were 57 Co ($t_{1/2}$: 271.7 d, 100.0% EC), 58 Co ($t_{1/2}$: 70.9 d, 14.9% 6 , 85.1% EC) and ⁵⁷Ni ($t_{1/2}$: 35.6 h, 43.6% β^+ , 56.4% EC), particularly when natural nickel targets were used for the production.89 The saturation yield of 55Co when natural nickel foils were bombarded with a beam energy of 16 MeV was 236 MBq (µA h)⁻¹ (i.e. 6.3 mCi (μ A h)⁻¹) at EOB with purity exceeding 97%.⁸⁹ ⁵⁵Co yields from 16 MeV proton beam bombardments of >99% ⁵⁸Ni-electroplated gold disk substrates resulted in 9.3 MBq (μA h)⁻¹ (i.e. 0.3 mCi (μ A h)⁻¹) with a purity exceeding 92%.⁸⁸

Product purification and target recovery. Column-based separation techniques have been used to isolate cobalt from the

nickel targets after heated dissolution with concentrated HCl.^{81,88,89} The first example used an AG1-X8 anion exchange resin^{81,89} which retained the cobalt product when the acidic target solution was passed through. Dilute HCl with concentrations ranging from 0.4–0.5 M (ref. 81 and 89) could be used to elute the cobalt product from the resin. Another stationary phase, DGA branched resin, ⁸⁸ was demonstrated to selectively release ⁵⁵Co upon elution with 3 M HCl. The overall separation efficiency for the process generally exceeded 90%. ^{88,89} If the method used for target preparation was the electroplating of enriched ⁵⁸Ni on a metal disk substrate, ⁵⁸Ni was recovered with a 94% efficiency from the spent target solution using a series of drying and chemical cleaning stages before finally being reconstituted as an electroplating solution. ⁸⁸

Summary. Table 5 summarizes key production and purification parameters for ⁵⁵Co not mentioned in Table 1.

Manganese: ^{52g}Mn

Applications. A considerable amount of interest in the use of 52g Mn ($t_{1/2}$: 5.6 d, 29.4% β^+ , 70.6% EC) in PET applications has developed since its first use as a myocardial perfusion PET agent in 1985.91 The radionuclide has been used in several preclinical imaging studies, including murine 4T1 xenografts, functional β-cells in type 1 and type 2 diabetes, and neural imaging in primates.22,92 The interest in 52gMn stems from its decay characteristics, ease of production, and its potential to act as a surrogate to non-invasively quantify MR contrast agent.93 The ^{52g}Mn radioisotope has a long half-life which facilitates late time-point studies up to 2 to 3 weeks following tracer administration, making it suitable for ImmunoPET applications. 1,94 Additionally, positron decay occurs at a low positron energy (β⁺ E_{max} : 575 keV), promoting high resolution imaging that is comparable to 18F.93 Despite its numerous advantages, caution is exercised when using ^{52g}Mn for PET applications since it has several high energy gamma emissions (i.e. 744, 935, and 1434

Table 4 Production and purification parameters for ⁶⁰Cu, ⁶¹Cu and ⁶⁴Cu

Radioisotope		⁶⁰ Cu, ⁶¹ Cu, ⁶⁴ Cu
Target material		Natural and enriched nickel (all), natural and enriched zinc (for ⁶¹ Cu only)
Product purity	⁶⁰ Cu	~98.8 to ~99.9%
Major impurities		⁶¹ Cu, ⁵⁵ Co, ⁵⁷ Co
Product purity	⁶¹ Cu	\sim 99.6% for 61 Ni(p,n) 61 Cu nuclear reaction; >95% for 64 Zn(p, α) 61 Cu nuclear reaction
Major impurities		⁵⁸ Co for ⁶¹ Ni(p,n) ⁶¹ Cu nuclear reaction; ⁶⁶ Ga, ⁶⁷ Ga, ⁶⁸ Ga for ⁶⁴ Zn(p,α) ⁶¹ Cu nuclear reaction
Product purity	⁶⁴ Cu	~95 to >99%
Major impurities		⁵⁵ Co, ⁵⁶ Co, ⁵⁷ Co, ⁵⁸ Co, ⁵⁷ Ni
Separation method	Ni	Anion exchange chromatography (AG 1-X8 resin)
		- Target dissolution: (a) HNO ₃ or (b) strong HCl
		- Ni target elution: (a) 0.2 N HCl in 96% methanol or (b) 6N HCl
		- Co impurity elution: (a) 0.3% HCl in 72% ethanol or (b) 4 N HCl
		- Copper elution: (a) 0.3 N HCl in 40% ethanol or (b) water
Product separation yield		95%
Target recovery yield		90%
Separation method	Zn	Ion exchange chromatography in series (AG 50W-X8 resin (cation) and AG 1-X8 resin (anion))
		- Target dissolution: 10 N HCl
		- (Cation exchange) Cu and Zn elution: 10 N HCl
		- (Anion exchange) Cu elution: 2 N HCl
		- (Anion exchange) Zn target elution: 0.5 N HCl
Product separation yield		
Target recovery yield		90%

RSC Advances Review

Table 5 Production and purification parameters for ⁵⁵Co

Radioisotope	⁵⁵ Co		
Target material	Natural and enriched nickel		
Product purity	92 to >97%		
Major impurities	⁵⁷ Co, ⁵⁸ Co, ⁵⁷ Ni		
Separation method	Anion exchange chromatography (AG1-X8 resin) - Target dissolution: concentrated HCl		
	- Co elution: 0.4–0.5 N HCl		
Product separation yield	>90%		
Target recovery yield	94%		

keV) coupled with prolonged residence in critical organs which require careful dosimetry studies prior to translation.

Production. 52gMn is primarily produced using the ⁵²Cr(p,n)^{52g}Mn nuclear reaction. ^{92,94–96} The reaction takes place within the 20 to 10 MeV beam energy range.93 The main target material used is natural chromium (isotopic composition: 4.35% 50 Cr, 83.79% 52 Cr, 9.50% 53 Cr, 2.37% 54 Cr) which can be loaded on to metal target substrates such as copper⁹⁵ and silver94 via electroplating or pressing.92,94,95 The natural chromium targets may also be a metal disk^{92,93} or foil.⁹⁶ The primary impurity produced during the reaction was 54 Mn ($t_{1/2}$: 312.2 d, 100.0% EC) via the 54Cr(p,n)54Mn nuclear reaction,92,94 however this impurity can be greatly reduced if 52Cr-enriched targets are used. ^{52m}Mn ($t_{1/2}$: 21.1 min, 96.6% β^+ , 1.6% EC, 1.8% IT) was also produced97 from the irradiation, however the radionuclide decays into 52gMn relatively quickly after its production. When chromium metal disks were bombarded with 16 MeV proton beams, a yield of 9.6 MBq (μ A h)⁻¹ (*i.e.* 0.26 mCi (μ A h)⁻¹) was reported at a purity level of 99.55%.93 For the composite, chromium/silver pressed targets bombarded at the same beam energy, a yield of 5 MBq (μ A h)⁻¹ (i.e. 0.1 mCi (μ A h)⁻¹) at a purity level of about 95% was reported.94 When natural chromium foils were irradiated with 12.5 MeV proton beams, a yield of 4.5 MBq (μ A h)⁻¹ (*i.e.* 0.12 mCi (μ A h)⁻¹) and a purity exceeding 99.0% was reported by Topping et al. (2013).

Product purification. The major method used to isolate manganese from the chromium targets is ion exchange chromatography. There are several different resins that can be used to carry out the isolation procedure. The most frequently used resin was the AG 1-X8 which required dissolution of the bombarded target in 11 to 12 M HCl. 93,96-98 After dissolution, the target solution was passed through the resin which selectively retained the manganese product, and elution was carried out using 0.1 M HCl. The separation efficiency of the process exceeded 97%.97 Apart from the AG 1-X8 resin, the 50W-X8 resin from Dowex or AG was also used to perform the separation, as discussed by Chaple and Lapi92 and Wooten et al.95 Methods for recovering the chromium target material have not been discussed, likely because recovery schemes tend not to be feasible when the large natural abundance of ⁵²Cr is considered.

Summary. Table 6 summarizes key production and purification parameters for ^{52g}Mn not mentioned in Table 1.

Niobium: 90Nb

Applications. A relative newcomer PET radionuclide, 90 Nb ($t_{1/}$ ₂: 14.6 h, 53.0% β^+ , 47.0% EC) is finding increasing consideration as a labelling agent in immunoPET applications due to close agreement between its half-life and the pharmacokinetics of peptides, antibody fragments and antibodies. 99,100 Additionally, 90Nb has a high probability of positron decay at moderate emission energies (β^+ $E_{\rm max}$: 1.5 MeV), which facilitates highresolution PET imaging.101 Protein labelling studies have been carried out as a preliminary step, including 90Nb-labelled monoclonal antibodies rituximab and bevacizumab in high yields. 102-104 90 Nb has also been used to label the peptide derivative DFO-succinyl-(D)Phe1-octreotide. 105 Although easily produced using low-energy cyclotrons, efficient separation methods ensuring quick isolation of 90Nb from bombarded target materials have not yet been established.99,105

Production. 90Nb is primarily produced via the 90Zr(p,n)90Nb nuclear reaction within the 19 to 7 MeV beam energy range. 99,105 However, ⁹⁰Nb could also be produced *via* the ⁹¹Zr(p,2n)⁹⁰Nb nuclear reaction when the incident beam energy exceeded 15 MeV.¹⁰⁵ Maximum ⁹⁰Nb production occurred at a beam energy of 13.5 MeV.¹⁰⁵ The target material for ⁹⁰Nb production was typically natural zirconium foils (isotopic composition: 51.45% ⁹⁰Zr, 11.22% ⁹¹Zr, 17.15% ⁹²Zr, 17.38% ⁹⁴Zr, 2.80% 96Zr),99,101-103,105 although the use of this target produced a significant number of impurities, making it unsuitable for clinical trial applications. 105 The primary impurities produced during the bombardment of natural zirconium were $^{89g/m}$ Nb ($t_{1/}$ 2: 2.0 h, 75.0% β⁺, 25.0% EC/66.0 min, 81.0% β⁺, 19.0% EC), ^{91m}Nb ($t_{1/2}$: 60.9 d, 96.6% IT, 3.4% EC), ^{92m}Nb ($t_{1/2}$: 10.2 d, 0.1% β⁺, 99.9% EC), ${}^{95g/m}$ Nb ($t_{1/2}$: 35.0 d, 100.0% β-/ $t_{1/2}$: 3.6 d, 5.6% β-, 94.4% IT), 96 Nb ($t_{1/2}$: 23.4 h, 100.0% β -), 87 Y ($t_{1/2}$: 79.8 h, 0.2% β ⁺, 99.8% EC) and ⁸⁹Zr ($t_{1/2}$: 78.4 h, 22.7.0% β^+ , 77.3% EC). ^{102,105} An alternative production route using ZrO₂ from enriched ⁹⁰Zr has been proposed by ref. 105, in which case the target preparation involved sedimentation of enriched ZrO₂ powder onto a copper substrate. Production using the 90ZrO2 targets had up to two orders of magnitude lower impurity levels. When three, 0.25 mm thick natural zirconium foils were irradiated with a 17.5 MeV proton beam, a 90 Nb yield of 145 MBq (μ A h) $^{-1}$ (*i.e.* 3.9 mCi (μ A h)⁻¹) was reported with a purity of 97% at EOB. ¹⁰² A yield of 596 MBq $(\mu A h)^{-1}$ (i.e. 16.1 mCi $(\mu A h)^{-1}$) with purity exceeding 95% was reported following the bombardment of

Table 6 Production and purification parameters for 529Mn

Radioisotope	^{52g} Mn
Target material	Natural chromium
Product purity	95 to 99.55%
Major impurities	⁵⁴ Mn, ^{52m} Mn
Separation method	Ion exchange chromatography
•	(AG1-X8 resin or other resins)
	- Target dissolution: 11 N HCl
	- Mn elution: 0.1 N HCl
Product separation yield	97%
Target recovery yield	n/a

three ⁹⁰ZrO₂-on-copper foil targets with an incident proton a s

beam energy of 11.9 MeV, 4 hours after EOB. 105

Product purification. There are two established methods that have been used to isolate the niobium product from postbombarded zirconium targets. The first method was described by Radchenko et al. 100,103 and required serial ion exchange chromatography separation. Irradiated zirconium targets were first dissolved in 28 M hydrofluoric acid and diluted to 21 M before loading on to the first ion exchange column. Cation exchange was performed by passing the solution through a DOWEX 50×8 resin (200-400 mesh) to retain trace metal ion impurities (i.e. copper and iron), colloids and undissolved particulate, while allowing the dissolved target material and product to pass through. After washing with concentrated HF, the emerging solution from the cation exchange stage was transferred to the second ion exchange stage. Anion exchange was performed using an AG 1 \times 8 resin (200–400 mesh) resin to retain the niobium product. To elute the niobium, a mixture of 1% H₂O₂ in 6 M HCl¹⁰¹ or 0.1 M oxalic acid¹⁰³ was used. If the former was used for elution, the H₂O₂ should be removed by

heating the eluate for 5 min at 120 °C. The overall efficiency of

the extraction procedure ranged from 93 to 95%. A second method was described by Radchenko et al., 101,102 which made use of a liquid-liquid extraction procedure. After placing into a small ice-water bath, the bombarded zirconium targets were dissolved in 48% HF (28 M). After complete target dissolution, 10 M HCl and saturated boric acid were added. More than 99% of the niobium product was then partitioned into chloroform using 0.02 M N-benzoyl-N-phenylhydroxylamine as a phase transfer catalyst. Liquid-liquid extraction was then performed with vigorous shaking for 20 min. After washing the organic phase with a mixture of 9 M HCl and 0.001 M HF and then 9 M HCl, respectively, the niobium product was reextracted from the organic phase using aqua regia with an extraction rate ranging from 90-95%. To increase the purity of the obtained ⁹⁰Nb product, the aqueous layer was subsequently passed through an anion exchange resin. The niobium containing solution was evaporated to dryness and the resulting residue was dissolved in a mixture of 0.25 M HCl and 0.1 M oxalic acid. Anion exchange was performed on the residue using a small Aminex A27 column, and the niobium product was eluted using a mixture of 6 M HCl and 0.01 M oxalic acid. The overall efficiency of the extraction procedure ranged from 76 to 81%.

In general, methods for recovering the zirconium target material have not been discussed, likely due to the lack of feasibility of any proposed recovery scheme given the relatively large natural abundance of ⁹⁰Zr.

Summary. Table 7 summarizes key production and purification parameters for ⁹⁰Nb not mentioned in Table 1.

Scandium: 44gSc

Applications. Favorable decay characteristics and the potential availability of a $^{44}{\rm Ti}/^{44}{\rm Sc}$ generator has brought $^{44}{\rm gSc}$ ($t_{1/2}$: 4.0 h, 94.3% β^+ , 5.7% EC) into clinical focus over the past decade. Scandium-44 is a trivalent radionuclide that is readily conjugated to peptides and proteins using common macrocyclic chelators such as DOTA and NOTA. This facilitates the growing number of preclinical and clinical PET studies reported, $^{106-110}$ and was exemplified by $^{44g}{\rm Sc}$ -labelling of PSMA-617 (*i.e.* peptidomimetic inhibitors) as an alternative for $^{68}{\rm Galabelling}.^{111}$ Due to the four-fold longer half-life, dosimetry measurements could be obtained 19 h post-injection to better match the pharmacokinetics of the $^{177}{\rm Lu}$ -labelled therapeutic. Additionally, $^{44}{\rm Sc}$ forms a true theranostic pairing with $^{47}{\rm Sc}.^{112}$

Production. There are many methods that can be used to produce 44gSc, ranging from the 44Ti/44gSc generator62,111 to small medical cyclotrons. 62,110,113,114 With respect to cyclotron production via solid targetry, one of the most common production routes is through the 44Ca(p,n)44g,mSc nuclear reaction. The process involves the use of solid targets formed from natural calcium (isotopic composition: 96.94% ⁴⁰Ca, 0.65% ⁴²Ca, 0.14% ⁴³Ca, 2.09% ⁴⁴Ca, >0.01% ⁴⁶Ca, 0.19% ⁴⁸Ca) and enriched 44Ca metal, 113 as well as enriched [44Ca]CaCO3 powders. 62,114 The nuclear reaction takes place over beam energies ranging from 18 to 6 MeV, with the reaction crosssection maximums between 13 and 10 MeV.114 The yield of ^{44g}Sc produced from the bombardment of >94% enriched [⁴⁴Ca] CaCO₃ powders at a beam energy of 11 MeV was 50 MBq (µA h)⁻¹ (i.e. 1.4 mCi (μ A h)⁻¹),¹¹⁴ while that obtained from the bombardment of natural calcium at a beam energy of 15.6 MeV

Table 7 Production and purification parameters for 90Nb

Radioisotope	⁹⁰ Nb
Target material	Natural and enriched zirconium oxide
Product purity	>95 to 97%
Major impurities	$^{89g/m}$ Nb, 91m Nb, 92m Nb, $^{95g/m}$ Nb, 96 Nb, 87 Y, 89 Zr
Separation method	1 Serial ion exchange chromatography (DOWEX 50 \times 8 resin (cation), AG 1 \times 8 resin (anion)) - Target dissolution: 28 M HF
	- (Cation exchange) 1st Nb elution: concentrated HF - (Anion exchange) 2nd Nb elution: 1% H ₂ O ₂ in 6 M HCl
Product separation yield	93 to 95%
Separation method	2 Liquid-liquid extraction - Target dissolution: 48% HF - Extraction solvents: 10 M HCl $^+$ saturated boric acid, 0.02 M <i>N</i> -benzoyl- <i>N</i> -phenylhydroxylamine in CHCl $_3$, aqua regia
Product separation yield	76 to 81%
Target recovery yield	n/a

RSC Advances Review

was 32 MBq $(\mu A h)^{-1}$ (i.e. 0.9 mCi $(\mu A h)^{-1}$) with a purity exceeding 95%. 110 It should be pointed out that targets with high concentrations of 44Ca perform poorly as solid targets due to their low electrical and heat conductivity properties. 110 The primary impurity produced during bombardment was $^{44\text{m}}$ Sc ($t_{1/}$ 2: 58.6 h, 98.8% IT, 1.2% EC) which has a negligible effect on PET studies when produced in small amounts. 110 44mSc has found new use as an in vivo generator in various pharmacokinetic studies^{62,113} due to its longer half-life and eventual decay into 44gSc. Other impurities produced during the proton irradiation of ⁴⁴Ca include ⁴⁷Sc ($t_{1/2}$: 3.3 d, 100.0% β-) and ⁴⁸Sc ($t_{1/2}$: 43.7 h, 100.0% β-), which were formed from trace amounts of ⁴⁸Ca *via* the ⁴⁸Ca(p,2n)⁴⁷Sc and ⁴⁸Ca(p,n)⁴⁸Sc nuclear reactions, respectively. 110,114 Small amounts of 43 Sc ($t_{1/2}$: 4.0 h, 88.1% β^+ , 11.9% EC)¹¹⁰ and ⁴⁶Sc ($t_{1/2}$: 83.8 d, 100.0% β -)⁶² have also been reported.

Product purification and target recovery. After acid dissolution, the scandium product can be isolated from irradiated calcium targets through column chromatography. However, the specific column and resin used varied with the type of target bombarded. With 44Ca metal, the target was first dissolved in concentrated HCl and then a UTEVA extraction resin was used to retain both the scandium product and the target material.110 The bulk target material was eluted with the 10 M HCl, while the scandium product was eluted subsequently with water, recovering \sim 80% of the ^{44g}Sc activity at EOB. When irradiating [⁴⁴Ca] CaCO₃, a chelating ion exchange resin (i.e. Chelex 100) was used114 after target dissolution in 0.1 M HCl. The resin retains both the scandium product and the target material, with the latter eluted first using 0.01 M HCl. The scandium product was removed using 1 M HCl with a separation efficiency exceeding 70%. A target-material recovery stage was further described in the work published by Krajewski et al.114 Briefly, the targetcontaining effluent was concentrated with ammonia. The new solution was subsequently heated to 170 °C to decompose

Table 8 Production and purification parameters for 44gSc

		·
Radioisotope		^{44g} Sc
Target material		Natural and enriched calcium, enriched calcium carbonate
Product purity		>95%
Major impurities		^{44m} Sc, ⁴⁷ Sc, ⁴⁸ Sc, ⁴³ Sc, ⁴⁶ Sc
Separation method	1	Ion exchange chromatography (UTEVA extraction resin) - Target dissolution: concentrated HCl - Ca elution: 10 M HCl - Sc elution: water
Product separation yield		80%
Target recovery yield		_
Separation method	2	Ion exchange chromatography (Chelex 100 resin) - Target dissolution: 0.1 M HCl - Sc elution: 0.01 M HCl - Ca elution: 1 M HCl
Product separation yield		70%
Target recovery yield		60%

NH₄Cl formed from the ammonia addition, and to evaporate any remaining water. 44Ca was recovered as 44CaO with a recovery efficiency of 60%, although the authors believed the small batch sizes processed strongly affected the recovery efficiency. Regardless, the addition of a recovery stage was worthwhile given the cost of 44Ca.62

Summary. Table 8 summarizes key production and purification parameters for ^{44g}Sc not mentioned in Table 1.

Technetium: 94mTc

Applications. The workhorse of nuclear medicine is the SPECT isotope $^{99\text{m}}$ Tc. ¹¹⁵ As a PET surrogate, $^{94\text{m}}$ Tc ($t_{1/2}$: 52 min, 70.2% β^+ , 29.8% EC) has seen limited use. Efflux transporter activity has been measured with 94mTc-sestamibi. The tracer was used in a preclinical multi-drug resistance study involving Pglycoprotein knock-out and wild-type mice, and showed delayed tracer clearance in the liver and kidney of the former group. 116 Other examples include examining cardiac function and estrogen receptor expression.117,118 A major application of ^{94m}Tc remains the quantitative assessment of novel ^{99m}Tc radiopharmaceuticals through in vivo PET studies.119 The limited adoption of 94mTc in PET can be attributed to several factors, with the most limiting being the prevalence of the highenergy gamma ray that is released during its decay. 120 Clinical applications using 94mTc for testing 99mTc radiopharmaceuticals are also limited by the relatively short half-life of 94mTc, 120 as well as the poor dosimetry of 94mTc which is seven-fold less favorable than that of 99mTc. 121

Production. 94mTc can be produced using the 94Mo(p,n) 94mTc nuclear reaction on small medical cyclotrons. 11,119-121 The reaction takes place within the 13 to 6 MeV energy range, 11,119 and has been carried out using both natural molybdenum foils (isotopic composition: 14.53% ⁹²Mo, 9.15% ⁹⁴Mo, 15.84% ⁹⁵Mo, 16.67% ⁹⁶Mo, 9.60% ⁹⁷Mo, 24.39% ⁹⁸Mo, 9.82% ¹⁰⁰Mo) and ⁹⁴Mo-enriched molybdenum oxide (*i.e.* MoO₃) pellets and powders. 120-122 When using 94Mo-enriched targets for production, the major impurity produced was 94g Tc ($t_{1/2}$: 293 min, 10.5% β⁺, 89.5% EC),¹¹⁹ especially when bombardment was conducted with beam energies equaling or exceeding 13 MeV. 120 When natural molybdenum was used for production, impurities such as $^{95g/m}$ Tc ($t_{1/2}$: 61.0 d, 0.4% β^+ , 96.1% EC, 3.9 IT/ $t_{1/2}$: 20.0 h, 100.0% EC), $^{96g/m}$ Tc ($t_{1/2}$: 4.3 d, 100.0% EC/ $t_{1/2}$: 51.5 min, 98.0% IT, 2.0% EC) and $^{99\text{m}}$ Tc ($t_{1/2}$: 6.0 h, 100.0% IT) were present in addition to 94gTc. 120-122 Despite the myriad of impurities formed, 94mTc production from natural molybdenum has been considered suitable for human radiopharmaceutical studies. 120 However, special attention should be given to 96mTc (which does not emit any imageable gamma rays)120 and 95Tc,123 which are both produced in significant amounts and have been shown to increase patient dose. When natural molybdenum foils were bombarded with an 11 MeV proton beam, a saturation yield of 111 MBq $(\mu A h)^{-1}$ (i.e. 3 mCi $(\mu A h)^{-1}$) was reported. However, a theoretical yield of 2000 MBq (μ A h)⁻¹ (i.e. 54 mCi $(\mu A h)^{-1}$) has been calculated for thick targets of enriched ⁹⁴Mo bombarded with beam energies ranging from 13 to 7 MeV.120,122

Product purification and target recovery. The primary method used to separate the technetium product from the metallic or oxide molybdenum target material was thermochromatographic dry distillation. 120,121 This requires heating of the irradiated targets in moist air,120 oxygen or helium.121 For molybdenum oxide targets heated to temperatures below 800 °C, volatile technetium species such as [94mTc]HTcO₄ and [94mTc]Tc₂O₇ sublime and were transported by the carrier gas until condensation temperatures (i.e. 250 to 350 °C) were reached. When heating was carried out at temperatures above 800 °C (i.e. 1090 °C (ref. 120)), both the technetium product and molybdenum target material sublimed. The molybdenum condenses first in the 600 to 800 °C temperature range, while the technetium product condenses at the cooler temperatures mentioned above. The condensed technetium product can be dissolved using hot NaOH and purified using a minimized alumina column. The entire separation process required approximately 25 minutes, and had an 80 to 85% product separation efficiency. The molybdenum target material was well isolated and could be easily recovered for immediate reuse with

Summary. Table 9 summarizes key production and purification parameters for $^{94\mathrm{m}}\mathrm{Tc}$ not mentioned in Table 1.

Titanium: 45Ti

a recovery efficiency exceeding 95%.

Review

Applications. Favorable decay characteristics has garnered increase consideration of 45 Ti ($t_{1/2}$: 3.08 h, 84.8% β^+ , 15.2% EC) as a PET imaging agent. These include a reasonable half-life and decaying to a stable daughter isotope, both of which are desirable features for PET radionuclides.¹²⁴ Additionally, ⁴⁵Ti has a high probability of positron decay at a moderate maximum positron energy ($\beta^+ E_{\text{max}}$: 1040). 92,124 Most positron decay events proceed directly to the ground state, making positron annihilation the primary source of gamma rays in the system. 124,125 These decay characteristics yield images that possess a high resolution.92 In addition to its favorable decay properties, 45Ti is also available to produce as discussed below. Despite its appeal, research on 45Ti radiolabeled tracers is limited as a result attributed to titanium's complicated chemistry and its high reactivity with oxygen. 92,126 Regardless, a few studies using 45Tiradiolabelled molecules exist. 45Ti has been used to label human serum albumin, phytate, DTPA and citrate for preclinical studies.125 A few bioconjugate studies have been completed including protein and peptide targeting vectors. Biodistributions studies in mice using [45Ti]transferrin observed high 45Ti uptake in the spleen and liver126 indicative of transchelation. Another recent example attached 45Ti to a PSMA-targeted peptidomimetic.126 In an interesting attempt to develop dual modality probes, chelate free mesoporous silica nanoparticles were labeled with ⁴⁵Ti for non-invasive in vivo quantification.127

Production. ⁴⁵Ti is produced *via* the ⁴⁵Sc(p,n)⁴⁵Ti nuclear reaction. ¹²⁸The reaction primarily takes place within the 16 to 8 MeV energy range, with a threshold energy of 2.9 MeV. ¹²⁸Regardless, a range restricted to 15 to 8 MeV was recommended to reduce the production of isotopic and non-isotopic impurities during bombardment. ¹²⁴The primary impurities produced during bombardment were ⁴⁴Ti ($t_{1/2}$: 59.1 years, 100.0% EC) from the ⁴⁵Sc(p,2n)⁴⁴Ti nuclear reaction, and ^{44g}Sc ($t_{1/2}$: 4.0 h, 94.3% β⁺, 5.7% EC) from the ⁴⁵Sc(p,pn)^{44g}Sc and ⁴⁵Sc(p,d)^{44g}Sc

Table 9 Production and purification parameters for ^{94m}Tc

^{94m} Tc			
Natural molybdenum, enriched molybdenum oxides			
_			
⁹⁴ Tc, ^{95g/m} Tc, 9 ^{6g/m} Tc, ^{99m} Tc			
Thermochromatographic dry distillation (500 to 1090 °C in moist air, O ₂ or He; hot NaOH for precipitate dissolution)			
80 to 85%			
>95%			

nuclear reactions. ¹²⁸ The target material was natural scandium (isotopic composition: 100.00% ⁴⁵Sc) foils. ^{92,124-126,128} A few values for ⁴⁵Ti yields have been reported in the literature. Vavere and Welch ¹²⁶ reported yields of 422 MBq (μ A h)⁻¹ (*i.e.* 11.4 mCi (μ A h)⁻¹) after bombarding 0.25 mm thick natural scandium foils with a 14.7 MeV proton beam. However, yields as low as 230 MBq (μ A h)⁻¹ (*i.e.* 6.2 mCi (μ A h)⁻¹) for bombardments at 11.8 MeV have been reported. ¹²⁷

Product purification. Cation-exchange chromatography has been used to isolate the titanium product from the scandium targets, and the method has been extensively described by Vavere et al. 125 and Vavere and Welch. 126 Post-bombarded targets were first dissolved in 6 N HCl, and the final solution was added to a cation exchange column filled with AG 50W-X8 resin (100–200 mesh). 145 Ti was then eluted with 6 N HCl, and this eluate was heated in the presence of a nitrogen stream to evaporate the HCl from the final product. Greater than 92% of the eluted 145 Ti product was obtained with a radionuclide purity of 99.8%. Methods for recovering the scandium target material have not been discussed as such methods would likely not be feasible due to the naturally high abundance of 145 Sc.

Summary. Table 10 summarizes key production and purification parameters for 45 Ti not mentioned in Table 1.

Yttrium: 86gY

Applications. As part of the original theranostic pairing, 129 86g Y ($t_{1/2}$: 14.7 h, 31.9% β^+ , 68.2% EC) is a residualizing radioisotope that has promising applications in radioimmunotherapy as an imaging compliment to its chemicallyidentical therapeutic counterpart, 90Y. Owing to its wellelucidated chelation chemistry, 86gY has been used to label several different antibodies, although the produced radiotracers have been limited to use in preclinical studies1 due to a few limitations. 86gY decays primarily by electron capture, generating several gamma emissions in the process. This negatively affects imaging quality and necessitates the use of corrections. 130 A second limitation is the accumulation of unbounded ^{86g}Y (due to conjugate dissociation or transchelation) in bone marrow, resulting in acute bone marrow toxicity. However, it should be mentioned that the risk of transchelation for ligands such as DOTA is low given the high thermodynamic and kinetic inertness of Y-DOTA chelates.131 Various peptides132,133 and antibodies134-137 have been radiolabeled with the intention of monitoring radioimmunotherapy. With respect to its utility as

RSC Advances Review

a the ranostic pair, the half-life of $^{86\mathrm{g}}\mathrm{Y}$ is short compared to $^{90}\mathrm{Y}$ and may limit the flexibility of radioimmunotherapy applications.1,138 Beyond immunoPET, 86Y has potential for use as a surrogate for gadolinium for non-invasive quantification of MR contrast agents.139

Production. 86gY is primarily produced via the 86Sr(p,n)86gY nuclear reaction, which also produces significant amounts of $^{86\text{m}}$ Y ($t_{1/2}$: 47.4 min, 99.3% IT, 0.4% β^+ , 0.3% EC), a shorter halflife impurity which quickly decays into ^{86g}Y. ⁶² ^{86g}Y has been produced from the bombardment of solid targets made from pressed, enriched 86SrCO3 (ref. 140-142) or 86SrO141 powders using proton beams of energies ranging from 15.1 to 11 MeV.140,142 Naturally, the yield of 86gY varied with the solid target material used as well as the specific irradiation conditions employed. When bombardments were carried out using 95.6% enriched 86SrCO3 solid target using a 15.1 MeV proton beam, an average 86g Y yield of 48 MBq (μ A h) $^{-1}$ (*i.e.* 1.3 mCi (μ A h) $^{-1}$) with a purity exceeding 99% was obtained. 62,140 Alternatively, bombardments carried out on 96.4% enriched 86SrO targets using a 14.5 MeV proton beam produced much higher 86gY yields of 166 MBq (μ A h)⁻¹ (*i.e.* 4.5 mCi (μ A h)⁻¹), with ^{86m}Y (220%), ${}^{87g/m}Y(t_{1/2}$: 79.8 h, 0.2% β^+ , 99.8% EC/ $t_{1/2}$: 13.3 h, 98.4% IT, 0.8 β^+ , 0.8% EC) (0.27%/0.43%) and ⁸⁸Y ($t_{1/2}$: 106.6 d, 0.2% β^{+} , 99.8% EC) (0.024%) being the primary impurities.^{62,141}

Product purification and target recovery. Multistageelectrolysis and filtration were two primary methods used to extract yttrium from post-bombardment strontium solid targets. The multistage-electrolysis procedure has been reported by Reischl et al.140 and Yoo et al.,141 and first required dissolution of the target material in 2.8 M HNO₃. To displace any oxygen and carbon dioxide dissolved in solution, the solution is sparged with an inert gas (i.e. argon) for 10 to 15 min before electrolysis began and continued through two electrolysis stages. The first electrolysis stage was carried out using a platinum plate cathode and anode. Yttrium was deposited on the cathode, followed by transfer to a platinum wire during a second electrolysis stage, where it was later removed and used for downstream labelling procedures. A simpler filtration method required dissolution of the targets in 6 M HCl, followed by the subsequent addition of 1 M NH₄OH. The resulting solution was then filtered under vacuum and washed with water to remove any residual strontium-containing liquid absorbed into the filter paper. Although the filtration-based separation

Table 10 Production and purification parameters for ⁴⁵Ti

Radioisotope	⁴⁵ Ti
Target material Product purity	Natural scandium
Major impurities Separation method	⁴⁴ Ti, ^{44g} Sc Cation exchange chromatography (AG 50W-X8 resin)
	- Target dissolution: 6 M HCl - Ti elution: 6 M HCl
Product separation yield Target recovery yield	>92% n/a

technique was considerably faster than the multistageelectrolysis technique, filtration-based separation suffered from a lower efficiency which affected overall yttrium yields. Multistage-electrolysis boasts separation efficiencies of about 97%, while the separation yield for filtration was about 88%.62 The strontium remaining in solution after electrolysis and filtration was available to be recovered for reuse. Depending on the chemical form of the strontium, a solution of (NH₄)₂CO₃ (ref. 140 and 142) or NH₄OH followed by the addition of saturated ammonium carbonate solution¹⁴¹ was used to precipitate the strontium in the form of 86SrCO3 with a recovery efficiency exceeding 90%. The 86SrCO3 can be converted to 86SrO through thermal decomposition if desired.141

Summary. Table 11 summarizes key production and purification parameters for ^{86g}Y not mentioned in Table 1.

Zinc: 63Zn

Applications. Zinc is the second most abundant transition metal in the human body being essential to numerous somatic processes, ranging from enzymatic stability to DNA regulation.143-145 Consequently, zinc dysregulation has been associated with many diseases, such as diabetes, Alzheimer's disease, and various cancers including breast, pancreatic and prostate cancer. 143,145,146 The critical role of zinc homeostasis in addition to its association to numerous diseases makes the development of non-invasive techniques for monitoring fluctuations in somatic zinc levels of great interest. 143,144 Of the many zinc radioisotopes, only three are positron-emitters, with 63 Zn ($t_{1/2}$: 38.5 min, 92.7% β^+ , 7.3% EC) showing the greatest promise due to its high probability for positron decay and ease of production.143 For conjugation, zinc only has one oxidation state which makes designing inert chelates much simpler. Despite its attractive properties, ⁶³Zn is limited by its comparatively short half-life, which restricts its viable application to about 2 hours.143 Regardless, 63Zn radiotracers are thought to be suitable for a variety of short investigative studies such as blood/ tissue zinc transport, pancreas and prostate transport kinetics, and blood-brain barrier investigations.143 A few clinical and preclinical PET studies have used a [63Zn]zinc citrate radiotracer to monitor zinc transport. 444 One preclinical study found that the radiotracer mainly accumulated in the gastrointestinal tract of mice, although a less significant accumulation in the brain of the animals was also reported. A clinical study comparing [63Zn]citrate uptake in brains of Alzheimer's disease patients and age-matched controls found no observed difference in uptake although the clearance of radioactivity was significantly slower in the patient group.147

Production. Although several nuclear reactions can be used to produce ⁶³Zn, the only reaction suitable for production using small medical cyclotrons is the 63Cu(p,n)63Zn nuclear reaction.144 This reaction takes place within the 16 to 5 MeV range using enriched 63Cu as well as natural copper (isotopic composition: 69.17% ⁶³Cu, 30.83% ⁶⁵Cu). In both cases, ⁶³Zn production was maximized in the 13 to 12 MeV energy range. The primary target material for the reactions were natural copper foils148 or natural copper that had been electroplated onto a suitable metal substrate such as gold.146 When a natural copper foil was bombarded with a 16 MeV proton beam, the

Table 11 Production and purification parameters for ^{86g}Y

Radioisotope		$^{86\mathrm{g}}\mathrm{Y}$
Target material Product purity Major impurities		Strontium oxides >99% ^{86m} Y, ^{87g/m} Y, ⁸⁸ Y
Separation method	1	Multistage electrolysis - Target dissolution: 2.8 M or 4% HNO ₃ - Platinum plate cathode and anode - Inert gas environment
Product separation yield		~97%
Separation method	2	Filtration - Target dissolution: 6 M HCl - Y precipitator: 1 M NH₄OH
Product separation yield Target recovery yield	>90%	~88%

reported 63 Zn yield was 2470 MBq (μA h) $^{-1}$ (*i.e.* 66.8 mCi (μA h) $^{-1}$) with a purity exceeding 99.9%. 148 The primary impurities generated during bombardment were 64 Cu ($t_{1/2}$: 12.7 h, 38.5% β $^-$, 10.8% β $^+$, 50.7% EC), 62 Zn ($t_{1/2}$: 9.2 h, 8.2% β $^+$, 91.8% EC), and 65 Zn ($t_{1/2}$: 243.9 d, 1.4% β $^+$, 98.6% EC). 144,148 The presence of the 65 Zn isotopic impurity is problematic for PET applications due to its long half-life. To limit the production of this impurity, bombardments at beam energies exceeding 11 MeV have been recommended. 148

Product purification. A method for isolating zinc from the irradiated natural copper targets is described by ref. 148. The natural copper target was first dissolved in concentrated HNO $_3$ before undergoing cation exchange with an AG 50W-X8 resin. The resin retained the zinc product, which can be eluted using a mixture of 0.05 N HCl and 85% acetone. The eluted zinc was obtained with a separation efficiency of 88.0%. Methods for recovering the copper target material have not been discussed as such methods would likely be impracticable due to the naturally high abundance of 63 Cu.

Summary. Table 12 summarizes key production and purification parameters for $^{63}{\rm Zn}$ not mentioned in Table 1.

Zirconium: 89Zr

Applications. The well matched half-life of 89 Zr ($t_{1/2}$: 78.4 h, 22.7% β^+ , 77.3% EC) with the pharmacokinetics of antibodies has led to more than 90 clinical studies, highlighted by the success of the ZEPHIR trial.4 These 89Zr-labelled antibodies are used to plan and monitor cancer treatments, visualize in vivo biodistribution, determine target expression, and conduct radiotherapy dosimetry. With the advancements in its production and labelling technology, 89Zr has been used to label numerous antibodies (i.e. HER1-targeted cetuximab, HER2targeted trastuzumab, VEGF-targeted bevacizumab, CD20targeted ibritumomab tiuxetan, transforming growth factorβ (TGF-β)-targeted fresolimumab, CD105-targeted TRC105 and PSMA-targeted 7E11) for both clinical and pre-clinical studies.¹ Most of these examples employed desferoxime (DFO) chelator which is less than ideal for zirconium149 with significant concentrations of unbound 89Zr found with certain radiotracers

such as ⁸⁹Zr-fresolimumab and ⁸⁹Zr-bevacizumab. This represents a major drawback of ⁸⁹Zr as free radiometal will accumulate in the bone and may negatively affect bone marrow health. ^{150,151} Ongoing efforts to develop improved ⁸⁹Zr chelates may address many of these concerns. ^{152–154}

Production. Although several nuclear reactions can be used to produce 89Zr, only the 89Y(p,n)89Zr reaction can be feasibly carried out on small medical cyclotrons. Natural yttrium (isotopic composition: 100.00% 89Y) targets can be bombarded with beam energies between 14 to 9 MeV, although the actual range for reasonable, high purity production is somewhat narrower.62 Bombardments with beam energies exceeding 11.6 MeV lead to the production of the long half-life contaminant, ⁸⁸Y ($t_{1/2}$: 106.6 d, 0.2% β^+ , 99.8% EC) formed *via* the ⁸⁹Y(p,pn)⁸⁸Y reaction, 155 while beam energies greater than 13 MeV resulted in the production of a second long half-life contaminant, ⁸⁸Zr ($t_{1/2}$: 83.4 d, 100.0% EC) which is inseparable from the final product and is formed via the ⁸⁹Y(p,2n)⁸⁸Zr reaction.⁶² Bombardments with beam energies below 10 MeV are not sufficient for 89Zr production. 62 Many different forms of yttrium targets have been investigated to produce 89Zr. Foil and pressed pellet targets were produced entirely from natural yttrium. Alternatively, targets can be composites composed of yttrium or an yttrium oxide (Y₂O₃) layered onto a suitable metal substrate such as copper using sputtering and deposition techniques. 156,157 A high purity yield of 58 MBq (μ A h)⁻¹ (*i.e.* 1.6 mCi (μ A h)⁻¹)^{64,158} has been reported in the literature for 89Zr production on yttrium metal targets in the aforementioned beam energy range. While the natural abundance of 89Y is monoisotopic it contains trace impurities of iron, titanium, and gadolinium. Proton interactions with those trace elements during bombardment form radionuclide impurities such as 48 V ($t_{1/2}$: 16.0 d, 49.9% β^+ , 50.1% EC), ¹⁵⁶Tb ($t_{1/2}$: 5.3 d, 100.0% EC), ⁶⁵Zn ($t_{1/2}$: 243.9 d, 1.4% β^+ , 98.6% EC) and 56 Co ($t_{1/2}$: 77.2 d, 19.7% β^+ , 80.3% EC) which negatively affect 89Zr antibody labelling and patient dosimetry.156

Product purification. To ensure high zirconium purity, column-based separation methods are generally utilized, with the most common being weak cation exchange. The irradiated yttrium targets were dissolved in strong (1 to 3 M) hydrochloric acid, and the solution was passed through a hydroxamate resin column. The hydroxamate column absorbed the zirconium ions in solution and later eluted using 1 M

Table 12 Production and purification parameters for ⁶³Zn

Radioisotope	⁶³ Zn		
Target material Product purity Major impurities	Natural copper >99.9% 64Cu, 62Zn, 63Zn, 65Zn		
Separation method	Cation exchange chromatography (AG 50-X8 resin) - Target dissolution: concentrated HNO ₃		
Product separation yield Target recovery yield	- Zn elution: 0.05 N HCl and 85% acetone 88% n/a		

oxalic acid with a separation efficiency exceeding 70%. Depending on the application, a second column-based separation and washing stage could be used to eliminate the oxalic acid from the complex it forms with zirconium since oxalic acid is highly toxic to the human body. When performed, the result was an zirconium product with a final purity exceeding 99.9%. 156-158 Methods for recovering the yttrium target material have not been discussed because recovery of natural Y targets is not practiced due to its economic characteristics vs. the purchase of new target material.

Summary. Table 13 summarizes key production and purification parameters for 89Zr not mentioned in Table 1.

Main group elements

Gallium: 66Ga, 68Ga

Applications. Due to its comparatively long half-life, 66 Ga ($t_{1/2}$: 9.5 h, 57.0% β^+ , 43.0% EC) has received some consideration in the field of PET for longer tracking of radiogallium. However only a few examples of ⁶⁶Ga PET radiotracers have been reported as the high energy emissions from its decay raises both patient and healthcare personnel safety concerns.¹ In one study, ⁶⁶Ga was used to label monoclonal antibodies (mAbs) to investigate tumor angiogenesis in animals. The study found that the radiotracer did not clear quickly from the bloodstream of the animals, resulting in moderate amounts of the radiotracer being found in the lungs, liver, heart, kidneys and spleen. 160 A second animal study demonstrated that unbound 66Ga accumulated in the bone and liver, pointing to metabolism or transchelation. ¹⁶¹ On the other hand, ⁶⁸Ga ($t_{1/2}$: 67.7 min, 88.9% β^{+} , 11.1% EC) has found extensive use as a small-molecule imaging tool within the last decade. 162-164 68Ga is particularly advantageous for the labelling of such compounds since its half-life is generally comparable to their pharmacokinetics. Another group of targeting molecules that can be radiolabeled using ⁶⁸Ga are peptides. These radiotracers are easy and inexpensive to produce and show quick blood clearance and tissue diffusivity. Most of the peptides that have been labelled are analogous to somatostatin, a regulatory protein primarily produced in the nervous and digestive systems. These analogues are able to interact with somatostatin receptors found in normal human tissues (i.e. the gastrointestinal tract, kidney, thyroid, spleen, brain, pancreas) and in a variety of

Table 13 Production and purification parameters for ⁸⁹Zr

Radioisotope	⁸⁹ Zr
Target material	Natural yttrium and its oxide
Product purity	>99.9%
Major impurities	⁸⁸ Y, ⁸⁸ Zr, ⁴⁸ V, ¹⁵⁶ Tb, ⁶⁵ Zn, ⁵⁶ Co
Separation method	Cation exchange chromatography (hydroxamate resin)
	- Target dissolution: 1 to 3 M HCl
	- Zr elution: 1 M oxalic acid
Product separation yield	70%
Target recovery yield	n/a

malignancies (i.e. neuroendocrine tumors, lymphomas, renal cell carcinomas, prostate cancer, breast cancer and small cell lung cancer), thus facilitating PET investigations. 68Ga has also been used to label melanocortin analogues for investigating melanocortin-receptor containing tissues (i.e. fibroblasts, leukocytes, keratinocytes, melanocytes and endothelial and antigen-presenting cells), and bombesin analogues for investigating bombesin-receptor containing tissue found in tumors (i.e. breast and prostate cancers). It is evident that 68Ga peptide radiotracers have been used in numerous preclinical and clinical studies, 165 including nearly 400 clinical investigations. The promising potential of ⁶⁸Ga radiopharmaceuticals have found clinical utility through successful imaging of PSMA, somatostatin receptors, and FAPI. 163,164,166

Production. 66Ga can be produced from the bombardment of both natural zinc (isotopic composition: 49.17% ⁶⁴Zn, 27.73% ⁶⁶Zn, 4.04% ⁶⁷Zn, 18.45% ⁶⁸Zn, 0.61% ⁷⁰Zn) and ⁶⁶Zn-enriched foils,167 or after electroplating onto gold or silver substrates.160 The radionuclide is primarily produced via the ⁶⁶Zn(p,n)⁶⁶Ga nuclear reaction at a minimum beam energy of 6 MeV,161 but irradiations are typically carried out at much higher energies (i.e. such as 9.8 MeV, 167 13 MeV, 160 14.5 MeV (ref. 167) and 15 MeV (ref. 161)). Yields of 511 MBq (μ A h)⁻¹ (*i.e.* 13.8 mCi (μ A h)⁻¹) with a purity of 99.96% have been achieved from the 14.5 MeV bombardment of 98.9% enriched 66Zn targets167 although higher yields of 700 MBq (μ A h)⁻¹ (*i.e.* 18.9 mCi (μ A h)⁻¹) have been reported elsewhere.64 The primary impurity produced during irradiation was 67 Ga ($t_{1/2}$: 3.3 d, 100.0% EC). 161,167

While ⁶⁸Ga has traditionally been produced with ⁶⁸Ge/⁶⁸Ga generators producing 1850 MBq and 3700 MBq of ⁶⁸Ga, cyclotrons have alternatively been used for its production via the proton bombardment of 68Zn-enriched targets. Recent progress using liquid targets has demonstrated modest production yields above 68Ge/68Ga generators. However solid targets show significant potential for much higher capacity production.168 Solid targets may be foils or zinc-coated metal backings (i.e. aluminum, gold or silver) that are generally prepared via electroplating or sputtering.169-171 The primary reaction governing the production of ⁶⁸Ga is the ⁶⁸Zn(p,n)⁶⁸Ga nuclear reaction, which takes place within the 14 to 11 MeV beam energy range. 62 Researchers have reported approximate yields of 1240 MBq (µA h)⁻¹ (i.e. 33.5 mCi (μ A h)⁻¹) from the bombardment of natural zinc targets at a beam energy of 12.5 MeV,171 and yields of 1380 MBq $(\mu A h)^{-1}$ (i.e. 37.3 mCi $(\mu A h)^{-1}$) for the bombardment of enriched >99% ⁶⁸Zn electroplated silver targets with a beam energy of 12.5 MeV.¹⁶⁹ A novel enriched zinc target design (backed with silver) irradiated at 13 MeV demonstrated a final yield of 1213 MBq (μ A h)⁻¹ (*i.e.* 32.8 mCi (μ A h)⁻¹) at end of separation (EOS) with a purity exceeding 99%. The major impurities produced from the reaction were 66 Ga ($t_{1/2}$: 9.5 h, 57.0% $β^+$, 43.0% EC) and ⁶⁷Ga ($t_{1/2}$: 3.3 d, 100.0% EC), and they are inseparable from the desired isotope.⁶² Measures can be taken to reduce 66/67Ga production during target irradiation including: (1) reduce the amounts of 66Zn and 67Zn in the targets by using highly enriched ⁶⁸Zn to limit the ⁶⁶Zn(p,n)⁶⁶Ga and ⁶⁷Zn(p,n)⁶⁷Ga nuclear reactions, and (2) limit the maximum

beam energy to 12 MeV to reduce the ⁶⁸Zn(p,2n)⁶⁷Ga nuclear reaction⁶² respectively. ¹⁶⁹

Product purification and target recovery. Gallium can be extracted from the zinc targets through two major methods. The first method made use of cation exchange chromatography where irradiated targets were dissolved in 10 to 12 M HCl and passed through a cation exchange resin, such as the AG 50W-X8 or AG 50W-X2, which retained both the zinc target material and gallium product. The zinc target material was then eluted using 10 M HCl, and was recovered with efficiencies ranging from 76 to 80%. The gallium product was subsequently eluted with 4 M HCl with an overall separation efficiency as high as 90%. 160,167,170 To increase the purity of the obtained gallium, a washing stage using 7 N HCl was carried out immediately before eluting the gallium product. 170 Alternatively, this procedure was carried out in a fully automated way using commercially available modules with separation efficiencies up to 80%. 169,171-173 Unreacted zinc target material was recovered from the 10 M HCl solution through electrolysis using a voltage of 5 V and a current of 1 A with efficiencies exceeding 76%.169

The second method for isolating gallium is liquid-liquid extraction. Preparation steps for this procedure involved dissolving the irradiated zinc targets in 12 M acid and diluting the resulting solution to 7 M with water. The dissolution was then subjected to a series of extraction and back-extraction stages using various solvents (*i.e.* diisopropyl ether, 7 M HCl and water) until gallium was obtained with the desired purity. Maximum separation efficiency for the gallium product was 79% and the recovery efficiency for the zinc target material exceeded 99%.

Summary. Table 14 summarizes key production and purification parameters for 66 Ga and 68 Ga not mentioned in Table 1. Arsenic: 72 As

Applications. ⁷²As ($t_{1/2}$: 26.0 h, 87.8% β^+ , 12.2% EC) is considered a promising PET radionuclide for several reasons including its long nuclear half-life which permits the radio-labeling of biomolecules with longer biological half-lives. ^{174,175}

The resulting radiotracers can be used in several extended biochemical and physiological process studies such as immunoimaging and receptor mapping. A second favorable characteristic arises from the unique soft Lewis acid properties of arsenic to covalently bond to thiol (or sulfhydryl) groups. 1,174,175 Theoretically, this allows arsenic's radioisotopes to directly label numerous biomolecules with little to no chemical modification.1,175 Several radioarsenic labeled antibodies and nanoparticles have been reported, although none have entered clinical use. 176-178 Finally, the positron emitting 72As provides a matched pair with ⁷⁷As ($t_{1/2}$: 38.8 h, 100% β^-) which will behave identically in vivo for imaging and radiotherapy, respectively.179 The theranostic advantage of the pairing makes up for the poor image resolution resulting from arsenic's large positron range (i.e. 3.6 mm in soft tissue). 58 Despite its favorable qualities however, research on the PET applications of ⁷²As has been slow as a result of the limited supply of isotopicallyenriched germanium, the primary material for the production of various arsenic radioisotopes, 1,175 although selenium has been used on occasion. 180 The limited supply of isotopicallyenriched germanium increases target costs which translates into an overall increase in ⁷²As production costs. ¹⁷⁵

Production. ⁷²As can be produced using a ⁷²Se/⁷²As generator, or using a solid target cyclotron.¹ With respect to the latter, ⁷²As can be produced using a variety of nuclear reactions such as ⁷²Ge(p,n)⁷²As, ⁷³Ge(p,2n)⁷²As, ⁷⁴Ge(p,3n)⁷²As and ⁷⁶Se (p,x)⁷²As. ^{180,181} Of the listed reactions, the most commonly used was the ⁷²Ge(p,n)⁷²As nuclear reaction which took place within the 18 to 8 MeV range, ¹⁷⁴ noting that ⁷²As production at beam energies exceeding 15 MeV contained a greater number of impurities in the final product. ¹⁷⁴ The targets used for ⁷²As production were typically ⁷²Ge-enriched germanium disks ¹⁷⁸ and ⁷²Ge-enriched germanium oxide that had been electroplated onto substrates made of copper ¹⁷⁴ and niobium. ¹⁷⁵ Additionally, natural germanium oxide ¹⁷⁴ or natural germanium (isotopic composition: 20.57% ⁷⁰Ge, 27.45% ⁷²Ge, 7.75% ⁷³Ge, 36.50% ⁷⁴Ge, 7.73% ⁷⁶Ge) foil ¹⁸² have also been used to produce

Table 14 Production and purification parameters for ⁶⁶Ga and ⁶⁸Ga

Radioisotope		⁶⁶ Ga, ⁶⁸ Ga
Target material	⁶⁶ Ga	Natural and enriched zinc
Product purity		>99.9%
Major impurities		⁶⁷ Ga
Target material	⁶⁸ Ga	Enriched zinc
Product purity		>99%
Major impurities		⁶⁶ Ga, ⁶⁷ Ga
Separation method	1	Cation exchange chromatography (AG 50W-X8 and AG 50W-X2 resins)
		- Target dissolution: 10 to 12 M HCl
		- Zn elution: 10 M HCl
		- Ga elution: 4 M HCl
Product separation yield		90%
Target recovery yield		76 to 80%
Separation method	2	Liquid-liquid extraction
•		- Target dissolution: 12 M HCl
		- Extraction solvents: Diisopropyl ether, 7 M HCl and water
Product separation yield		79%
Target recovery yield		>99%

RSC Advances Review

⁷²As in other studies. The primary impurities produced during bombardment were ⁷¹As $(t_{1/2}: 65.3 \text{ h}, 28.3\% \text{ β}^+, 71.7\% \text{ EC})$, ⁷⁴As $(t_{1/2}: 17.8 \text{ d}, 34.0\% \text{ β}^-, 29.0\% \text{ β}^+, 37.09\% \text{ EC})$, ⁷⁶As $(t_{1/2}: 26.2 \text{ h}, 100.0\% \text{ β}^-)$, ⁶⁹Ge $(t_{1/2}: 39.1 \text{ h}, 24.0\% \text{ β}^+, 76.0\% \text{ EC})$ and ⁶⁷Ga $(t_{1/2}: 3.3 \text{ d}, 100.0\% \text{ EC})$ (175,178,182). The ⁷²As production yield for >96% enriched germanium oxide electroplated onto a niobium substrate and bombarded with 16.1 MeV protons was 90 MBq (μA h)⁻¹ (*i.e.* 2.4 mCi (μA h)⁻¹), with purity exceeding 99%.¹⁷⁸ The theoretical ⁷²As yield for natural germanium oxide electroplated onto a copper substrate and bombarded with a proton beam energy of 15 MeV to 8 MeV was 60 MBq (μA h)⁻¹ (*i.e.* 1.6 mCi (μA h)⁻¹).¹⁷⁴

Product purification and target recovery. Methods for isolating arsenic from the germanium targets have been described extensively in Enferadi et al., 174 Ellison et al. 175,178 and Guin et al. 183 In general, the methods required dissolution of the germanium targets using solutions of 6 M NaOH or hot aqua regia, followed by the addition of 6 to 10 N HCl. The addition of the HCl was necessary to convert the germanium metal to GeCl₄, which is significantly more volatile than the metallic arsenic product. Thirty percent hydrogen peroxide was then added to oxidize the arsenic to the As(v) state. The final dissolution was evaporated to near dryness, after which distillation was performed on the resulting residue. About 97% of the ⁷²As was left behind as residue from the distillation, and then further purified through ion exchange chromatography after dissolution in 10 M HCl. Anion exchange was carried out by passing the arsenic solution through a Bio-Rad AG 1 \times 8 resin (200-400 mesh), which retained the arsenic product as well as any residual germanium and gallium impurities. The arsenic could be collected by eluting with 10 M HCl, and the procedure had a separation efficiency of 93%, resulting in an overall As(v) separation efficiency of about 90%. However, if it is desirous to have the arsenic in the As(III) state instead of its As(v) state, SPE can be carried out subsequently. The SPE procedure had an efficiency of 57% and after its application, the overall separation efficiency of the As(III) product was 51%. Recovery of the germanium target material could be achieved by treating the acidic condensate from the dissolution stage with 6 M NaOH.

Table 15 Production and purification parameters for ⁷²As

	·
Radioisotope	⁷² As
Target material	Natural and enriched germanium and their oxides
Product purity	>99%
Major impurities	⁷¹ As, ⁷⁴ As, ⁷⁶ As, ⁶⁷ Ga, ⁶⁹ Ge
Separation method	Distillation, Anion exchange chromatography and SPE
	- (Distillation) target dissolution: 6 M NaOH or hot aqua regia $^+$ 6 to 10 N HCl $^+$ 30% H $_2$ O $_2$ - (Chromatography) target distillation: 10 M
	HCl
	- As elution: 10 M HCl
Product separation yield	>90% As(v), ~51% As(iii)
Target recovery yield	${\sim}60\%$

This neutralized the condensate, and converted $GeCl_4$ to GeO which could be easily reduced to metallic germanium when sufficiently heated. The overall recovery efficiency reported by Ellison *et al.*¹⁷⁸ was about 60%, however it should be emphasized that higher recovery efficiencies could be achieved if the recovery process was optimized.

Summary. Table 15 summarizes key production and purification parameters for ⁷²As not mentioned in Table 1.

Conclusion

Given the surge in clinical use and interest in several metallic radioisotopes, solid target systems for small (≤24 MeV) medical cyclotrons are rapidly evolving to enable large-scale production with consistent yield, composition and quality. With this, many factors need to be considered when choosing to develop inhouse radiometal production capabilities, including (i) the variability in medical cyclotron design (i.e. beam energy, current and machine configuration); (ii) target isotope availability; (iii) quality/quantity variations when compared to alternative, noncyclotron production routes, and (iv) the intended application of the radioisotope. While many of the metallic radioisotopes discussed herein are being developed as imaging agents unto themselves, several have the potential to be theragnostic partners to a range of chemically diverse therapeutic radioisotopes, and require considerations in chemical compatibility and physical/biological half-life. Of those diagnostic radioisotopes with theragnostic applications, the community will likely see near-term adoption of cyclotron-produced ⁶⁸Ga and ⁸⁹Zr, and a resurgence of interest in ⁶⁴Cu. Radioisotopes with elementidentical theragnostic application such as 86Y, 44Sc and 124I may encounter increases in use as long as their production and/ or recycling methodologies can be sufficiently optimized. Yet others, such as cyclotron-produced 99mTc, may emerge as important enablers for those regions in which supply via noncyclotron-based alternatives remain problematic.

Nomenclature and units

Alpha particle

	r
β^-	Beta emission
β^+	Positron emission
d	Days
EC	Electron capture
$E_{\rm max}$	The endpoint energy (i.e. maximum energy) of an
	emitted positron
EOB	End of bombardment
h	Hours
IT	Isomeric transition
keV	Kiloelectron volts
MBq	Megabecquerels
MeV	Megaelectron volts
μA	Microamperes
mCi	Millicuries
min	Minutes
M	Molar (i.e. mols of acid per liter)

Review RSC Advances

n Neutron

N Normal (i.e. moles of dissociated H⁺ ions per liter)

°C Degrees celsius

PET Positron emission tomography

p Positron

SPECT Single photon computed tomography

SPE Solid phase extraction

 $t_{1/2}$ Half-life γ Gamma ray

Conflicts of interest

There are no conflicts of interest to declare.

References

- 1 Y. Zhou, K. E. Baidoo and M. W. Brechbiel, Mapping Biological Behaviors by Application of Longer-Lived Positron Emitting Radionuclides, *Adv. Drug Delivery Rev.*, 2013, 65(8), 1098–1111.
- 2 A. Boschi, P. Martini, V. Costa, A. Pagnoni and L. Uccelli, Interdisciplinary tasks in the cyclotron production of radiometals for medical applications The case of ⁴⁷Sc as example, *Molecules*, 2019, 24(3), 444.
- 3 S. Reddy and M. Robinson, ImmunoPET In Cancer Models, *Semin. Nucl. Med.*, 2010, **40**(3), 182–189.
- 4 E. Boros and J. Holland, Chemical aspects of metal ion chelation in the synthesis and application antibody-based radiotracers, *J. Labelled Compd. Radiopharm.*, 2018, **61**(9), 652–671.
- 5 G. Stöcklin and V. W. Pike, *Radiopharmaceuticals for Positron Emission Tomography-Methodological Aspects*, Springer Science & Business Media, Vol. 24, 1993.
- 6 M. Sajjad and R. M. Lambrecht, Cyclotron targetry for medical radioisotope production, *Nucl. Instrum. Methods Phys. Res., Sect. B*, 1989, 40, 11001104.
- 7 H. F. Valdovinos, S. Graves, P. Ellison, T. Barnhart and R. J. Nickles, Earth, air, fire and water: A targetry quartet, AIP Conf. Proc., 2017, 1845.
- 8 S. M. Qaim, Target development for medical radioisotope production at a cyclotron, *Nucl. Instrum. Methods Phys. Res.*, 1989, **282**(1), 289–295.
- 9 International Atomic Energy Agency, Cyclotron produced radionuclides: physical characteristics and production methods International Atomic Energy Agency, Vienna, Austria, 2009.
- 10 C. J. Anderson and R. Ferdani, Copper-64 radiopharmaceuticals for PET imaging of cancer: Advances in preclinical and clinical research, *Cancer Biother.Radiopharm.*, 2009, 24(4), 379–393.
- 11 M. Fassbender, A. F. Novgorodov, F. Rösch and S. M. Qaim, Excitation Functions of ⁹³Nb(3He,xn)^{93m,g,94m,g,95m,g}Tc-Processes from Threshold up to 35 MeV: Possibility of Production of ^{94m}Tc in High Radiochemical Purity using a Thermochromatographic Separation Technique, *Radiochim. Acta*, 1994, **65**(4), 215–222.

12 H. Büyükuslu, A. Kaplan, G. Yıldırım, A. Aydin, E. Tel and M. Bölükdemir, Production cross sections of medical 110,111 In radionuclides, *Kerntechnik*, 2010, 73(3), 103–108.

- 13 T. Kostelnik and C. Orvig, Radioactive main group and rare earth metals for imaging and therapy, *Chem. Rev.*, 2018, 119(2), 902–956.
- 14 A. Rahman and A. Awal, Production of ¹⁴⁹Tb, ¹⁵²Tb, ¹⁵⁵Tb and ¹⁶¹Tb from gadolinium using different light-particle beams, *J. Radioanal. Nucl. Chem.*, 2020, 323(2), 731–740.
- 15 A. Klein, F. Rösch and S. Qaim, Investigation of ⁵⁰Cr(d,n)⁵¹Mn and natCr(p, x)⁵¹Mn processes with respect to the production of the positron emitter ⁵¹Mn, *Radiochim. Acta*, 2000, **88**(5), 253–264.
- 16 E. Boros and A. Packard, Radioactive transition metals for imaging and therapy, *Chem. Rev.*, 2018, **119**(2), 870–901.
- 17 A. H. Asad, S. V. Smith, S. Chan, C. M. Jeffery, L. Morandeau and R. I. Price, Cyclotron production of ⁶¹Cu using natural Zn & enriched ⁶⁴Zn targets, in *AIP Conference Proceedings*, 2012, pp. 91–5.
- 18 T. Z. Wong, J. L. Lacy, N. A. Petry, T. C. Hawk, T. A. Sporn, M. W. Dewhirst, et al., PET of hypoxia and perfusion with ⁶²Cu-ATSM and ⁶²Cu-PTSM using a ⁶²Zn/⁶²Cu generator, Am. J. Roentgenol., 2008, 190(2), 427–432.
- 19 E. Aluicio-Sarduy, N. Thiele, K. Martin, B. Vaughn, J. Devaraj, A. Olson, et al., Establishing radiolanthanum chemistry for targeted nuclear medicine applications, *Chemistry*, 2020, 26(6), 1238.
- 20 E. Aluicio-Sarduy, T. Barnhart, J. Weichert, R. Hernandez and J. Engle, Cyclotron produced ¹³²La as a PET imaging surrogate of therapeutic ²²⁵Ac, *J. Nucl. Med.*, 2021, **62**(7), 1012–1015.
- 21 E. Boros and A. B. Packard, Radioactive Transition Metals for Imaging and Therapy, *Chem. Rev.*, 2018, **119**(2), 870–901.
- 22 E. Aluicio-Sarduy, P. Ellison, T. Barnhart, W. Cai, R. Nickles and J. Engle, PET radiometals for antibody labeling, *J. Labelled Compd. Radiopharm.*, 2018, **61**(9), 636–651.
- 23 H. Coenen and J. Ermert, Expanding PET-applications in life sciences with positron emitters beyond fluorine-18, *Nucl. Med. Biol.*, 2021, **92**, 241–269.
- 24 H. Coenen, M. Harmand, G. Kloster and G. Stöcklin, 15-(p[⁷⁵Br] bromophenyl) pentadecanoic Acid: Pharmacokinetics
 and Potential as Heart Agent, *J. Nucl. Med.*, 1981, 22(10),
 891–896.
- 25 O. De Jesus, G. Van Hoffaert, D. Glock, L. Goldber and A. Friedman, Synthesis of a radiobrominated analog of SCH 23390, a selfctive dopamine D1/DA1 antagonist, *J. Labelled Compd. Radiopharm.*, 1986, 23(9), 919–925.
- 26 S. Moerlein and G. Stoecklin, Synthesis of high specific activity [⁷⁵Br]-and [⁷⁷Br] Bromperidol and tissue distribution studies in the rat. Journal of medicinal chemistry, *J. Med. Chem.*, 1985, **28**(9), 1319–1324.
- 27 S. Moerlein, P. Laufer, G. Stöcklin, G. Pawlik, K. Wienhard and W. Heiss, Evaluation of ⁷⁵Br-labelled butyrophenone neuroleptics for imaging cerebral dopaminergic receptor areas using positron emission tomography, *Eur. J. Nucl. Med.*, 1986, **12**(4), 211–216.

28 J. Rice, N. Hussain and E. Lavoie, Synthesis of [methoxy-14C] eugenol, J. Labelled Compd. Radiopharm.,

RSC Advances

1987, 24(9), 1043-1049. 29 G. Kloster, P. Laufer, W. Wutz and G. Stöcklin, 75,77 Br-and

- 123 I-analogues of D-glucose as potential tracers for glucose utilisation in heart and brain, Eur. J. Nucl. Med., 1983, 8(6), 237-241.
- 30 D. J. Rowland, T. J. McCarthy and M. J. Welch, Radiobromine for imaging and therapy, in Handbook of Radiopharmaceuticals: Radiochemistry and Applications, 2002, pp. 441-465.
- 31 P. McQuade, D. J. Rowland, J. S. Lewis and M. J. Welch, Positron-Emitting Isotopes Produced on Biomedical Cyclotrons, Curr. Med. Chem., 2005, 12(7), 807-818.
- 32 M. Kassiou, C. Loc'h, M. Bottlaender, K. Mardon, M. Ottaviani, C. Coulon, et al., (+)-[⁷⁶Br] A-69024: a nonbenzazepine radioligand for studies of dopamine D1 receptors using PET, Nucl. Med. Biol., 2002, 29(3), 295-302.
- 33 C. Foged, C. Halldin, C. Loc'h, B. Mazière, P. Karlsson, M. Mazière, et al., ¹¹C-and ⁷⁶Br-labelled NNC 22-0010, selective dopamine D1 receptor radioligands for PET, Nucl. Med. Biol., 1996, 23(6), 837-844.
- 34 C. Lundkvist, C. Loc'h, C. Halldin, M. Bottlaender, M. Ottaviani, C. Coulon, et al., Characterization of bromine-76-labelled 5-bromo-6-nitroquipazine for PET studies of the serotonin transporter, Nucl. Med. Biol., 1999, 26(5), 501-507.
- 35 L. Lang, W. Li, H. Jia, D. Fang, S. Zhang, X. Sun, et al., New methods for labeling RGD peptides with bromine-76, Theranostics, 2011, 1, 341.
- 36 S. Cho, L. Ravasi, L. Szajek, J. Seidel, M. Green, H. Fine, et al., Evaluation of ⁷⁶Br-FBAU as a PET reporter probe for HSV1-tk gene expression imaging using mouse models of human glioma, J. Nucl. Med., 2005, 46(11), 1923-1930.
- 37 S. Watanabe, H. Hanaoka, J. Liang, Y. Iida, K. Endo and N. Ishioka, PET Imaging of Norepinephrine Transporter-⁷⁶Br-meta-Expressing **Tumors** Using Bromobenzylguanidine, J. Nucl. Med., 2010, 51(9), 1472-1479.
- 38 R. Rossin, D. Berndorff, M. Friebe, L. M. Dinkelborg and M. J. Welch, Small-animal PET of tumor angiogenesis using a 76Br-labeled human recombinant antibody fragment to the ED-B domain of fibronectin, J. Nucl. Med., 2007, 48(7), 1172-1179.
- 39 N. Vaiseman, G. Koren and P. Pencharz, Pharmacokinetics of oral and intravenous bromide in normal volunteers, J. Toxicol. Clin. Toxicol., 1986, 24(5), 403-413.
- 40 C. Lang, D. Habs, K. Parodi and P. Thirolf, Sub-millimeter nuclear medical imaging with high sensitivity in positron emission tomography using $\beta^+ \gamma$ coincidences, J. Instrum., 2014, 9(1), P01008.
- 41 M. Sitarz, J. Cussonneau, T. Matulewicz and F. Haddad, Radionuclide candidates for β^+ γ coincidence PET: an overview, Appl. Radiat. Isot., 2020, 155, 108898.
- 42 D. Wilbur and M. Adam, Radiobromine and radioiodine for medical applications, Radiochim. Acta, 2019, 107(9-11), 1033-1063.

- 43 Progress in Radiopharmacy. Progress in Radiopharmacy. ed. P Cox, S Mather, C Sampson and C Lazarus, Springer Science & Business Media; 2012.
- 44 Z. Kovács, G. Blessing, S. M. Qaim and G. Stöcklin, Production of ⁷⁵Br via the ⁷⁶Se(p,2n)⁷⁵Br reaction at a compact cyclotron, Int. J. Appl. Radiat. Isot., 1985, 36(8), 635-642.
- 45 S. M. Qaim, Recent developments in the production of ¹⁸F, ^{75,76,77}Br and ¹²³I, *Int. J. Radiat. Appl. Instrum. Appl. Radiat.* Isot., 1986, 37(8), 803-810.
- 46 D. J. Schlyer, Production of Radionuclides in Acclerators, in Handbook of radiopharmaceuticals, radiochemistry and applications, 2003. pp. 1-70.
- 47 K. Breunig, I. Spahn, S. Spellerberg and H. H. Coenen, Production of no-carrier-added radiobromine: New nickel selenide target and optimized separation by dry distillation, Radiochim. Acta, 2015, 103(5), 397-402.
- 48 V. Tolmachev, A. Lövqvist, L. Einarsson, J. Schultz and H. Lundqvist, Production of ⁷⁶Br by a low-energy cyclotron, Appl. Radiat. Isot., 1998, 49(12), 1537-1540.
- 49 A. Bruskin, I. Sivaev, M. Persson, H. Lundqvist, J. Carlssona, S. Sjoberg, et al., Radiobromination of monoclonal antibody using potassium [76Br](4 isothiocyanatobenzylammonio)-bromo-decahydro-closo-dodecaborate (Bromo-DABI), Nucl. Med. Biol., 2004, 31(2), 205-211.
- 50 S. Mahajan and C. Divgi, The role of iodine-124 positron emission tomography in molecular imaging, Clin. Transl. Imaging, 2016, 4(4), 297-306.
- 51 J. A. O'Donoghue, P. M. Smith-Jones, J. L. Humm, S. Ruan, D. A. Pryma, A. A. Jungbluth, et al., 124 I-huA33 antibody uptake is driven by A33 antigen concentration in tissues from colorectal cancer patients imaged by immuno-PET, J. Nucl. Med., 2011, 52(12), 1878–1885.
- 52 I. Verel, G. W. M. Visser, O. C. Boerman, J. E. M. Van Eerd, R. Finn, R. Boellaard, et al., Long-lived positron emitters zirconium-89 and iodine-124 for scouting of therapeutic radioimmunoconjugates with PET, Cancer Biother.Radiopharm., 2003, 18(4), 655-661.
- 53 G. C. Jayson, J. Zweit, A. Jackson, C. Mulatero, P. Julyan, M. Ranson, et al., Molecular imaging and biological evaluation of HuMV833 anti-VEGF antibody: Implications for trial design of antiangiogenic antibodies, J. Natl. Cancer Inst., 2002, 94(19), 1484-1493.
- 54 A. M. S. Braghirolli, W. Waissmann, J. B. Da Silva and G. R. Dos Santos, Production of iodine-124 and its applications in nuclear medicine, Appl. Radiat. Isot., 2014, 90, 138-148.
- 55 H. Coenen, K. Dutschka, S. Müller, L. Geworski, J. Farahati and C. Reiners, Nca radiosynthesis of [123,124 I] β -CIT, plasma analysis and pharmacokinetic studies with SPECT and PET, Nucl. Med. Biol., 1995, 22(8), 977-984.
- 56 C. Zechmann, A. Afshar-Oromieh, T. Armor, J. Stubbs, W. Mier, B. Hadaschik, et al., Radiation dosimetry and first therapy results with a 124 I/131 I-labeled small molecule (MIP-1095) targeting PSMA for prostate cancer therapy, Eur. J. Nucl. Med. Mol. Imag., 2014, 41(7), 1280-1292.

57 C. Foss, D. Plyku, A. Ordonez, J. Sanchez-Bautista, H. Rosenthal, I. Minn, *et al.*, Biodistribution and radiation dosimetry of ¹²⁴I-DPA-713, a PET radiotracer for macrophage-associated inflammation, *J. Nucl. Med.*, 2018, 59(11), 1751–1756.

- 58 L. Carter, A. Kesner, E. Pratt, V. Sanders, A. Massicano, C. Cutler, et al., The impact of positron range on PET resolution, evaluated with phantoms and PHITS Monte Carlo simulations for conventional and non-conventional radionuclides, Mol. Imag. Biol., 2020, 22(1), 73–84.
- 59 N. Shah, H. Herzog, C. Weirich, L. Tellmann, J. Kaffanke, L. Caldeira, et al., Effects of magnetic fields of up to 9.4 T on resolution and contrast of PET images as measured with an MR-BrainPET, PLoS One, 2014, 4, e95250.
- 60 S. D. Wilbur, S. W. Hadley, M. D. Hylarides, P. G. Abrams, P. A. Beaumier, A. C. Morgan, *et al.*, Development of a stable radioiodinating reagent to label monoclonal antibodies for radiotherapy of cancer, *J. Nucl. Med.*, 1989, 30(2), 216–226.
- 61 M. Berman, L. Braverman, J. Burke, L. De Groot, K. McCormack, T. Oddie, *et al.*, Summary of Current Radiation Dose Estimates to Humans from ¹²³I, ¹²⁴I, ¹²⁵I, ¹²⁶I, ¹³⁰I, ¹³¹I, and ¹³²I as Sodium Iodide, *J. Nucl. Med.*, 1975, **16**(12), 1214–1217.
- 62 M. A. Synowiecki, L. R. Perk and J. F. W. Nijsen, Production of novel diagnostic radionuclides in small medical cyclotrons, *EJNMMI Radiopharm. Chem*, 2018, 3(1), 3.
- 63 L. Koehler, K. Gagnon, S. McQuarrie and F. Wuest, Iodine-124: A promising positron emitter for organic PET chemistry, *Molecules*, 2010, **15**(4), 2686–2718.
- 64 S. M. Qaim, Nuclear data for production and medical application of radionuclides: Present status and future needs, *Nucl. Med. Biol.*, 2017, 44, 31–49.
- 65 D. W. McCarthy, L. A. Bass, P. D. Cutler, R. E. Shefer, R. E. Klinkowstein, P. Herrero, *et al.*, High purity production and potential applications of copper-60 and copper-61, *Nucl. Med. Biol.*, 1999, 26(4), 351–358.
- 66 S. Lapi, J. Lewis and F. Dehdashti, Evaluation of hypoxia with copper-labeled diacetyl-bis (N-methylthiosemicarbazone), *Semin. Nucl. Med.*, 2015, 45(2), 177–185.
- 67 M. Conti and E. Lars, Physics of pure and non-pure positron emitters for PET: a review and a discussion, *EJNMMI Phys*, 2016, 3(1), 1–7.
- 68 W. Ping Li, L. A. Meyer, D. A. Capretto, C. D. Sherman and C. J. Anderson, Receptor-binding, biodistribution, and metabolism studies of ⁶⁴Cu-DOTA-cetuximab, a PETimaging agent for epidermal growth-factor receptorpositive tumors, *Cancer Biother.Radiopharm.*, 2008, 23(2), 158–171.
- 69 M. Lewis, C. Boswell, R. Laforest, T. Buettner, D. Ye, J. Connett, et al., Conjugation of monoclonal antibodies with TETA using activated esters: biological comparison of ⁶⁴Cu-TETA-1A3 with ⁶⁴Cu-BAT-2IT-1A3, Cancer Biother.Radiopharm., 2001, 16(6), 483–494.
- 70 B. Gutfilen, S. Souza and G. Valentini, Copper-64: a real theranostic agent, *Drug Des., Dev. Ther.*, 2018, **12**, 3235.

- 71 N. Smith, D. Bowers and D. Ehst, he production, separation, and use of ⁶⁷Cu for radioimmunotherapy: a review, *Appl. Radiat. Isot.*, 2012, **70**(10), 2377–2383.
- 72 P. Rowshanfarzad, M. Sabet, A. Reza Jalilian and M. Kamalidehghan, An overview of copper radionuclides and production of ⁶¹Cu by proton irradiation of natZn at a medical cyclotron, *Appl. Radiat. Isot.*, 2006, **64**(12), 1563– 1573.
- 73 P. Rajec, V. Csiba, M. Leporis, M. Štefečka, E. L. Pataky, M. Reich, et al., Preparation and characterization of nickel targets for cyclotron production of ⁶⁴Cu, J. Radioanal. Nucl. Chem., 2010, 286(3), 665–670.
- 74 C. M. Jeffery, S. V. Smith, A. H. Asad, S. Chan and R. I. Price, Routine production of copper-64 using 11.7MeV protons, *AIP Conf. Proc.*, 2012, **1509**(1), 84–90.
- 75 M. A. Avila-Rodriguez, J. A. Nye and R. J. Nickles, Simultaneous production of high specific activity ⁶⁴Cu and ⁶¹Co with 11.4 MeV protons on enriched ⁶⁴Ni nuclei, *Appl. Radiat. Isot.*, 2007, **65**(10), 1115–1120.
- 76 D. W. McCarthy, R. E. Shefer, R. E. Klinkowstien, L. A. Bass, W. H. Margeneau, C. S. Cutler, *et al.*, Efficient production of high specific activity ⁶⁴Cu using a biomedical cyclotron, *Nucl. Med. Biol.*, 1997, 24(1), 35–43.
- 77 A. Obata, S. Kasamatsu, D. W. McCarthy, M. J. Welch, H. Saji, Y. Yonekura, et al., Production of therapeutic quantities of ⁶⁴Cu using a 12 MeV cyclotron, Nucl. Med. Biol., 2003, 30(5), 535–539.
- 78 J. De Reuck, K. Paemeleire, P. Santens, K. Strijckmans and I. Lemahieu, Cobalt-55 positron emission tomography in symptomatic atherosclerotic carotid artery disease: Borderzone versus territorial infarcts, *Clin. Neurol. Neurosurg.*, 2004, 106(2), 77–81.
- 79 J. De Reuck, P. Santens, J. Keppens, J. De Bleecker, K. Strijckmans, P. Goethals, *et al.*, Cobalt-55 positron emission tomography in recurrent ischaemic stroke, *Clin. Neurol. Neurosurg.*, 1999, 101(1), 15–18.
- 80 H. Jansen, R. Dierckx, J. Hew, A. Paans, J. Minderhoud and J. Korf, Positron emission tomography in primary brain tumours using cobalt-55, *Nucl. Med. Commun.*, 1997, 18(8), 734–740.
- 81 T. Mastren, B. Marquez, D. Sultan, E. Bollinger, P. Eisenbeis, T. Voller, et al., Cyclotron production of high Specific activity ⁵⁵Co and in vivo evaluation of the stability of ⁵⁵Co metal-chelate-peptide complexes, Mol. Imag., 2015, 14(10), 7290.
- 82 J. Garousi, K. Andersson, J. Dam, B. Olsen, B. Mitran, A. Orlova, *et al.*, The use of radiocobalt as a label improves imaging of EGFR using DOTA-conjugated Affibody molecule, *Sci. Rep.*, 2017, 7(1), 1–10.
- 83 J. Dam, B. Olsen, C. Baun, P. Høilund-Carlsen and H. Thisgaard, Vivo Evaluation of a bombesin analogue labeled with Ga-68 and Co-55/57, *Mol. Imag. Biol.*, 2016, **18**(3), 368–376.
- 84 P. Goethals, A. Volkaert, C. Vandewielle, R. Dierckx and N. Lameire, ⁵⁵Co-EDTA for renal imaging using positron emission tomography (PET): a feasibility study, *Nucl. Med. Biol.*, 2000, 27(1), 77–81.

85 B. Mitran, H. Thisgaard, U. Rosenström, J. Dam, M. Larhed, V. Tolmachev, et al., High contrast PET imaging of GRPR

expression in prostate cancer using cobalt-labeled bombesin antagonist RM26, Contrast Media Mol. Imaging, 2017, 1-10.

RSC Advances

- 86 M. Al-abyad, M. N. H. Comsan and S. M. Qaim, Excitation functions of proton-induced reactions on with particular reference to the production of ⁵⁷Co, Appl. Radiat. Isot., 2009, 67(1), 122-128.
- 87 A. G. Wain and I. L. Jenkins, Functions for the bombardment, J. Inorg. Nucl. Chem., 1970, 32(1970), 1419-
- 88 H. F. Valdovinos, R. Hernandez, S. Graves, P. A. Ellison, T. E. Barnhart, C. P. Theuer, et al., Cyclotron production and radiochemical separation of ⁵⁵Co and ^{58m}Co from ⁵⁴Fe, ⁵⁸Ni and ⁵⁷Fe targets, Appl. Radiat. Isot., 2017, 130, 90-101.
- 89 H. F. Valdovinos, S. Graves, T. Barnhart and R. J. Nickles, ⁵⁵Co separation from proton irradiated metallic nickel, AIP Conf. Proc., 2014, 1626(1), 217-220.
- 90 P. Goethals, A. Volkaert, C. Vandewielle, R. Dierckx and N. Lameire, ⁵⁵Co-EDTA for renal imaging using positron emission tomography (PET): A feasibility study, Nucl. Med. Biol., 2000, 27(1), 77-81.
- 91 M. Daube and R. Nickles, Development of myocardial perfusion tracers for positron emission tomography, Int. J. Nucl. Med. Biol., 1985, 12(4), 303-314.
- 92 I. F. Chaple and S. E. Lapi, Production and Use of the First-Row Transition Metal PET Radionuclides 43,44Sc, 52Mn, and ⁴⁵Ti, J. Nucl. Med., 2018, **59**(11), 1655–1659.
- 93 C. M. Lewis, S. A. Graves, R. Hernandez, H. F. Valdovinos, T. E. Barnhart, W. Cai, et al., 52Mn production for PET/ MRI tracking of human stem cells expressing divalent metal transporter 1 (DMT1), Theranostics, 2015, 5(3), 227-239.
- 94 S. A. Graves, R. Hernandez, J. Fonslet, C. G. England, H. F. Valdovinos, P. A. Ellison, et al., Novel Preparation Methods of 52Mn for ImmunoPET Imaging, Physiol. Behav., 2015, 26(10), 2118-2124.
- 95 A. L. Wooten, B. C. Lewis, R. Laforest, S. V. Smith and S. E. Lapi. Cyclotron Production and PET/MR Imaging of ⁵²Mn, in *Proceedings of the 15th International Workshop on* Targetry and Target Chemistry. 2014.
- 96 G. J. Topping, P. Schaffer, C. Hoehr, T. J. Ruth and V. Sossi, Manganese-52 positron emission tomography tracer characterization and initial results in phantoms and in vivo, Med. Phys., 2013, 40(4), 042502-2-042502-8.
- 97 J. Fonslet, S. Tietze, A. I. Jensen, S. A. Graves and G. W. Severin, Optimized procedures for manganese-52: Production, separation and radiolabeling, Appl. Radiat. Isot., 2017, 121, 38-43.
- 98 A. I. Jensen, G. W. Severin, A. E. Hansen, F. P. Fliedner, R. Eliasen, L. Parhamifar, et al., Remote-loading of liposomes with manganese-52 and in vivo evaluation of the stabilities of 52Mn-DOTA and 64Cu-DOTA using radiolabelled liposomes and PET imaging, J. Controlled Release, 2018, 269, 100-109.

- 99 S. Busse, J. Brockmann and F. Rösch, Radiochemical separation of no-carrier-added radioniobium from zirconium targets for application of 90Nb-labelled compounds, Radiochim. Acta, 2002, 90(7), 411-416.
- 100 V. Radchenko, S. Busse and F. Roesch, Desferrioxamine as an appropriate chelator for 90Nb: Comparison of its complexation properties for M-Df-Octreotide (M=Nb, Fe, Ga, Zr), Nucl. Med. Biol., 2014, 41(9), 721-727.
- 101 V. Radchenko, D. V. Filosofov, O. K. Bochko, N. A. Lebedev, A. V. Rakhimov, H. Hauser, et al., Separation of 90Nb from zirconium target for application in immuno-pet, Radiochim. Acta, 2014, 102(5), 433-442.
- 102 V. Radchenko, H. Hauser, M. Eisenhut, D. J. Vugts, G. A. Van Dongen and F. Roesch, 90Nb - A potential PET nuclide: Production and labeling of monoclonal antibodies, Radiochim. Acta, 2012, 100(11), 857-864.
- 103 V. Radchenko, D. V. Filosofov, J. Dadakhanov, D. V. Karaivanov, A. Marinova, A. Baimukhanova, et al., Direct flow separation strategy, to isolate no-carrier-added ⁹⁰Nb from irradiated Mo or Zr targets, Radiochim. Acta, 2016, 104(9), 625-634.
- 104 A. De La Fuente, V. Radchenko, T. Tsotakos, C. Tsoukalas, M. Paravatou-Petsotas, A. Harris, et al., Conjugation, labelling and in vitro/in vivo assessment of an anti-VEGF monoclonal antibody labelled with niobium isotopes, J. Radioanal. Nucl. Chem., 2018, 318(3), 1991-1997.
- 105 S. Busse, F. Rösch and S. M. Qaim, Cross section data for the production of the positron emitting niobium isotope ⁹⁰Nb via the 90Zr(p,n)-reaction, Radiochim. Acta, 2002, 90(1), 1-5.
- 106 E. Koumarianou, N. Loktionova, M. Fellner, F. Roesch, O. Thews, D. Pawlak, et al., 44Sc-DOTA-BN [2-14] NH2 in comparison to ⁶⁸Ga-DOTA-BN [2-14] NH2 in pre-clinical investigation. Is 44Sc a potential radionuclide for PET?, Appl. Radiat. Isot., 2012, 70(12), 2669-2676.
- 107 H. Honarvar, C. Müller, S. Cohrs, S. Haller, K. Westerlund, A. Karlström, et al., Evaluation of the first 44Sc-labeled Affibody molecule for imaging of HER2-expressing tumors, Nucl. Med. Biol., 2017, 45, 15-21.
- 108 A. Khawar, E. Eppard, J. Sinnes, F. Roesch, H. Ahmadzadehfar, S. Kürpig, et al., [44Sc] Sc-PSMA-617 biodistribution and dosimetry in patients with metastatic castration-resistant prostate carcinoma, Clin. Nucl. Med., 2018, 43(5), 323-330.
- 109 G. Orteca, J. Sinnes, S. Rubagotti, M. Iori, P. Capponi, M. Piel, et al., Gallium-68 and scandium-44 labelled radiotracers based on curcumin structure linked to bifunctional chelators: Synthesis and characterization of potential PET radiotracers, J. Inorg. Biochem., 2020, 204, 110954.
- 110 R. Hernandez, H. F. Valdovinos, Y. Yang, R. Chakravarty, H. Hong, T. E. Barnhart, et al., 44Sc: An attractive isotope for peptide-based PET imaging, Mol. Pharm., 2014, 11(8), 2954-2961.
- 111 E. Eppard, A. de la Fuente, M. Benešová, A. Khawar, R. A. Bundschuh, F. C. Gärtner, et al., Clinical translation and first in-human use of [44Sc]Sc-PSMA-617 for pet

imaging of metastasized castrate-resistant prostate cancer, *Theranostics*, 2017, 7(18), 4359.

- 112 K. Siwowska, P. Guzik, K. Domnanich, J. Monné Rodríguez, P. Bernhardt, B. Ponsard, et al., Therapeutic potential of ⁴⁷Sc in comparison to ¹⁷⁷Lu and ⁹⁰Y: Preclinical investigations, *Pharmaceutics*, 2019, 11(8), 424.
- 113 V. Radchenko, C. A. Meyer, J. W. Engle, C. M. Naranjo, G. A. Unc, T. Mastren, *et al.*, Separation of ⁴⁴Ti from proton irradiated scandium by using solid-phase extraction chromatography and design of ^{44Ti/44}Sc generator system, *J. Chromatogr. A*, 2016, **1477**, 39–46.
- 114 S. Krajewski, I. Cydzik, K. Abbas, A. Bulgheroni, F. Simonelli, U. Holzwarth, *et al.*, Cyclotron production of ⁴⁴Sc for clinical application, *Radiochim. Acta*, 2013, **101**(5), 333–338
- 115 S. Banerjee, M. Pillai and N. Ramamoorthy, Evolution of Tc-99m in diagnostic radiopharmaceuticals, *Semin. Nucl. Med.*, 2001, 31(4), 260–277.
- 116 H. Bigott, D. McCarthy, F. Wüst, J. Dahlheimer, D. R. Piwnica-Worms and M. Welch, Production, processing and uses of ^{94m}Tc. Journal of Labelled Compounds and Radiopharmaceuticals, *J. Labelled Compd. Radiopharm.*, 2001, 44(S1), S119–S121.
- 117 C. Stone, B. Christian, R. Nickles and S. Perlman, Technetium 94m-labeled methoxyisobutyl isonitrile: dosimetry and resting cardiac imaging with positron emission tomography, *J. Nucl. Cardiol.*, 1994, 1(5), 425–433.
- 118 H. Bigott, E. Parent, L. Luyt, J. Katzenellenbogen and M. Welch, Design and synthesis of functionalized cyclopentadienyl tricarbonylmetal complexes for technetium-94m PET imaging of estrogen receptors, *Bioconjugate Chem.*, 2005, 16(2), 255–264.
- 119 C. D. Illan and B. W. Wieland, Evaluation of a recoil-escape fiber target using 94Mo (p,n) 94mTc to produce 94TcO4-precursor for radiolabeled compounds useful in positron emission tomography, Duke University Medical Center, Durham NC, 2001.
- 120 S. M. Qaim, Production of high purity ^{94m}Te for positron emission tomography studies, *Nucl. Med. Biol.*, 2000, 27(4), 323–328.
- 121 B. T. Christian, R. J. Nickles, C. K. Stone, T. L. Mulnix and J. Clark, Improving the radionuclidic purity of ^{94m}Tc for PET imaging, *Appl. Radiat. Isot.*, 1995, **46**(2), 69–73.
- 122 F. Rösch and S. M. Qaim, Nuclear Data Relevant to the Production of the Positron Emitting Technetium Isotope ^{94m}Tc via the ⁹⁴Mo(p,n)-reaction, *Radiochim. Acta*, 1993, **62**(3), 115–122.
- 123 X. Hou, J. Tanguay, K. Buckley, P. Schaffer, F. Bénard, T. J. Ruth, *et al.*, Molybdenum target specifications for cyclotron production of ^{99m}Tc based on patient dose estimates, *Phys. Med. Biol.*, 2015, **61**(2), 542–553.
- 124 M. Sadeghi, M. Enferadi and H. Nadi, ⁴⁵Ti, a candidate for positron emission tomography: Study of the cyclotron production, *Radiochemistry*, 2011, 53(4), 411–414.
- 125 A. L. Vavere, R. Laforest and M. J. Welch, Production, processing and small animal PET imaging of titanium-45, *Nucl. Med. Biol.*, 2005, 32(2), 117–122.

- 126 A. Vavere and M. Welch, Preparation, biodistribution, and small animal PET of ⁴⁵Ti-transferrin, *J. Nucl. Med.*, 2005, **46**(4), 683–690.
- 127 F. Chen, H. F. Valdovinos, R. Hernandez, S. Goel, T. E. Barnhart and W. Cai, Intrinsic radiolabeling of Titanium-45 using mesoporous silica nanoparticles, *Acta Pharmacol. Sin.*, 2017, 38(6), 907–913.
- 128 S. Kuhn, I. Spahn, B. Scholten and H. H. Coenen, Positron and γ -ray intensities in the decay of ⁴⁵Ti, *Radiochim. Acta*, 2015, **103**(6), 403–409.
- 129 F. Rösch, S. Qaim and G. Stöcklin, Production of the positron emitting radioisotope ⁸⁶Y for nuclear medical application, *Appl. Radiat. Isot.*, 1993, 44(4), 677–681.
- 130 T. K. Nayak, K. Garmestani, K. E. Baidoo, D. E. Milenic and M. W. Brechbiel, PET imaging of tumor angiogenesis in mice with VEGF-A-targeted ⁸⁶Y-CHX-A'''-DTPAbevacizumab, *Int. J. Cancer*, 2011, 128(4), 920–926.
- 131 T. Wadas, E. Wong, G. Weisman and C. Anderson, Coordinating radiometals of copper, gallium, indium, yttrium, and zirconium for PET and SPECT imaging of disease, *Chem. Rev.*, 2010, **110**(5), 2858–2902.
- 132 T. Clifford, C. Boswell, G. Biddlecombe, J. Lewis and M. Brechbiel, Validation of a Novel CHX-A "Derivative Suitable for Peptide Conjugation: Small Animal PET/CT Imaging Using Yttrium-86-CHX-A "-Octreotide, *J. Med. Chem.*, 2006, 49(14), 4297–4304.
- 133 L. Wei, X. Zhang, F. Gallazzi, Y. Miao, X. Jin, M. Brechbiel, et al., Melanoma imaging using ¹¹¹In-, ⁸⁶Y-and ⁶⁸Ga-labeled CHX-A "-Re (Arg11) CCMSH, Nucl. Med. Biol., 2009, 36(4), 345–354.
- 134 H. Chong, K. Garmestani, D. Ma, D. Milenic, T. Overstreet and M. Brechbiel, Synthesis and Biological Evaluation of Novel Macrocyclic Ligands with Pendent Donor Groups as Potential Yttrium Chelators for Radioimmunotherapy with Improved Complex Formation Kinetics, *J. Med. Chem.*, 2002, 45(46), 3458–3464.
- 135 C. Kang, X. Sun, F. Jia, H. Song, Y. Chen, M. Lewis, *et al.*, Synthesis and preclinical evaluation of bifunctional ligands for improved chelation chemistry of ⁹⁰Y and ¹⁷⁷Lu for targeted radioimmunotherapy, *Bioconjugate Chem.*, 2012, 23(9), 1775–1782.
- 136 L. Koi, R. Bergmann, K. Brüchner, J. Pietzsch, H. Pietzsch, M. Krause, *et al.*, Radiolabeled anti-EGFR-antibody improves local tumor control after external beam radiotherapy and offers theragnostic potential, *Radiother. Oncol.*, 2014, 110(2), 362–369.
- 137 T. Nayak, K. Garmestani, K. Baidoo, D. Milenic and M. Brechbiel, Preparation, biological evaluation, and pharmacokinetics of the human anti-HER1 monoclonal antibody panitumumab labeled with ⁸⁶Y for quantitative PET of carcinoma, *J. Nucl. Med.*, 2010, 51(6), 942–950.
- 138 S. Walrand, R. Barone, S. Pauwels and F. Jamar, Experimental facts supporting a red marrow uptake due to radiometal transchelation in ⁹⁰Y-DOTATOC therapy and relationship to the decrease of platelet counts, *Eur. J. Nucl. Med. Mol. Imag.*, 2011, 38(7), 1270–1280.

139 M. Le Fur, N. Rotile, C. Correcher, V. Clavijo Jordan, A. Ross, C. Catana, *et al.*, Yttrium-86 Is a Positron Emitting Surrogate of Gadolinium for Noninvasive Quantification of Whole-Body Distribution of Gadolinium-Based Contrast Agents, *Angew. Chem. Int. Ed.*, 2020, 59(4), 1474–1478.

RSC Advances

- 140 G. Reischl, F. Rösch and H. J. Machulla, Electrochemical separation and purification of yttrium-86, *Radiochim. Acta*, 2002, **90**(4), 225–228.
- 141 J. Yoo, L. Tang, T. A. Perkins, D. J. Rowland, R. Laforest, J. S. Lewis, *et al.*, Preparation of high specific activity ⁸⁶Y using a small biomedical cyclotron, *Nucl. Med. Biol.*, 2005, 32(8), 891–897.
- 142 M. A. Avila-Rodriguez, J. A. Nye and R. A. Nickles, Production and separation of non-carrier-added ⁸⁶Y from enriched ⁸⁶Sr targets, *Appl. Radiat. Isot.*, 2008, **66**(1), 9–13.
- 143 T. R. DeGrado, M. K. Pandey, J. F. Byrne, H. P. Engelbrecht, H. Jiang, A. B. Packard, *et al.*, Preparation and preliminary evaluation of ⁶³Zn-zinc citrate as a novel PET imaging biomarker for zinc, *J. Nucl. Med.*, 2014, 55(8), 1348–1354.
- 144 M. Rostampour, M. Aboudzadeh, M. Sadeghi and S. Hamidi, Theoretical assessment of production routes for ⁶³Zn by cyclotron, *J. Radioanal. Nucl. Chem.*, 2016, **309**(2), 677–684.
- 145 T. R. DeGrado, B. J. Kemp, M. K. Pandey, H. Jiang, T. M. Gunderson, L. R. Linscheid, *et al.*, First PET imaging studies with ⁶³Zn-zinc citrate in healthy human participants and patients with Alzheimer disease, *Mol. Imag.*, 2016, **15**, 1–10.
- 146 M. Rostampour, M. Sadeghi, M. Aboudzadeh, K. Yousefi and S. Hamidi, Investigation of the thermal performance of natCu target for ⁶³Zn production, *Appl. Radiat. Isot.*, 2018, **141**, 1–4.
- 147 T. DeGrado, B. Kemp, M. Pandey, H. Jiang, T. Gunderson, L. Linscheid, et al., First PET imaging studies with ⁶³Znzinc citrate in healthy human participants and patients with Alzheimer disease, Mol. Imag., 2016, 15, 1536012116673793.
- 148 M. Rostampour, M. Sadeghi, M. Aboudzadeh, S. Hamidi, N. Soltani, F. B. Novin, *et al.*, Experimental study and simulation of ⁶³Zn production via proton induce reaction, *Appl. Radiat. Isot.*, 2018, **136**, 32–36.
- 149 S. Heskamp, R. Raavé, O. Boerman, M. Rijpkema, V. Goncalves and F. Denat, ⁸⁹Zr-immuno-positron emission tomography in oncology: state-of-the-art ⁸⁹Zr radiochemistry, *Bioconjugate Chem.*, 2017, **28**(9), 2211–2223.
- 150 T. H. Oude Munnink, M. E. A. Arjaans, H. Timmer-Bosscha, C. P. Schröder, J. W. Hesselink, S. R. Vedelaar, *et al.*, PET with the ⁸⁹Zr-labeled transforming growth factor-β antibody fresolimumab in tumor models, *J. Nucl. Med.*, 2011, 52(12), 2001–2008.
- 151 W. B. Nagengast, E. G. De Vries, G. A. Hospers, N. H. Mulder, J. R. De Jong, H. Hollema, *et al.*, In vivo VEGF imaging with radiolabeled bevacizumab in a human ovarian tumor xenograft, *J. Nucl. Med.*, 2007, **48**(8), 1313–1319.

- 152 J. Yoon, B. Park, E. Ryu, Y. An and S. Lee, Current Perspectives on ⁸⁹Zr-PET Imaging, *Int. J. Mol. Sci.*, 2020, 21(12), 4309.
- 153 N. Bhatt, D. Pandya and T. Wadas, Recent advances in zirconium-89 chelator development. Molecules, *Molecules*, 2018, 23(3), 638.
- 154 J. Holland, Predicting the thermodynamic stability of zirconium radiotracers, *Inorg. Chem.*, 2020, **59**(3), 2070–2082.
- 155 A. M. Dabkowski, S. J. Paisey, M. Talboys and C. Marshall, Optimization of cyclotron production for radiometal of zirconium 89, *Acta Phys. Pol.*, *A*, 2015, 127(5), 1479–1482.
- 156 A. Kasbollah, P. Eu, S. Cowell and P. Deb, Review on production of ⁸⁹Zr in a medical cyclotron for PET radiopharmaceuticals, *J. Nucl. Med. Technol.*, 2013, **41**(1), 35–41.
- 157 M. J. O'Hara, N. J. Murray, J. C. Carter and S. S. Morrison, Optimized anion exchange column isolation of zirconium-89 (⁸⁹Zr) from yttrium cyclotron target: Method development and implementation on an automated fluidic platform, *J. Chromatogr. A*, 2018, **1545**, 48–58.
- 158 G. Severin, J. Engle, T. Barnhart and R. Nickles, ⁸⁹Zr Radiochemistry for Positron Emission Tomography, *Med. Chem.*, 2011, 7(5), 389–394.
- 159 W. E. Meijs, J. D. M. Herscheid, H. J. Haisma, R. Wijbrandts, F. van Langevelde, P. J. Van Leuffen, *et al.*, Production of highly pure no-carrier added ⁸⁹Zr for the labelling of antibodies with a positron emitter, *Appl. Radiat. Isot.*, 1994, **45**(12), 1143–1147.
- 160 J. W. Engle, H. Hong, Y. Zhang, H. F. Valdovinos, D. V. Myklejord, T. E. Barnhart, *et al.*, Positron emission tomography imaging of tumor angiogenesis with a ⁶⁶Galabeled monoclonal antibody, *Mol. Pharm.*, 2012, 9(5), 1441–1448.
- 161 Ö. Ugur, P. J. Kothari, R. D. Finn, P. Zanzonico, S. Ruan, I. Guenther, et al., Ga-66 labeled somatostatin analogue DOTA-DPhe1-Tyr3-octreotide as a potential agent for positron emission tomography imaging and receptor mediated internal radiotherapy of somatostatin receptor positive tumors, Nucl. Med. Biol., 2002, 29(2), 147–157.
- 162 M. Khan, S. Khan, S. El-Refaie, Z. Win, D. Rubello and A. Al-Nahhas, Clinical indications for gallium-68 positron emission tomography imaging, *Eur. J. Surg. Oncol.*, 2009, 35(6), 561–567.
- 163 M. Perera, N. Papa, M. Roberts, M. Williams, C. Udovicich, I. Vela, et al., Gallium-68 prostate-specific membrane antigen positron emission tomography in advanced prostate cancer—updated diagnostic utility, sensitivity, specificity, and distribution of prostate-specific membrane antigen-avid lesions: a systematic review and meta-, Eur. Urol., 2020, 77(4), 403–417.
- 164 C. Kratochwil, P. Flechsig, T. Lindner, L. Abderrahim, A. Altmann, W. Mier, *et al.*, ⁶⁸Ga-FAPI PET/CT: tracer uptake in 28 different kinds of cancer, *J. Nucl. Med.*, 2019, **60**(6), 801–805.
- 165 F. Giesel, C. Kratochwil, T. Lindner, M. Marschalek, A. Loktev, W. Lehnert, et al., ⁶⁸Ga-FAPI PET/CT:

biodistribution and preliminary dosimetry estimate of 2 DOTA-containing FAP-targeting agents in patients with various cancers, J. Nucl. Med., 2019, 60(3), 386-392.

- 166 U. Hennrich and M. Benešová, [68Ga] Ga-DOTA-TOC: The First FDA-Approved ⁶⁸Ga-Radiopharmaceutical for PET Imaging, Pharmaceuticals, 2020, 13(3), 38.
- 167 M. R. Lewis, D. E. Reichert, R. Laforest, W. H. Margenau, R. E. Shefer, R. E. Klinkowstein, et al., Production and purification of gallium-66 for preparation of tumortargeting radiopharmaceuticals, Nucl. Med. Biol., 2002, 29(6), 701-706.
- 168 M. E. Rodnick, C. Sollert, D. Stark, M. Clark, A. Katsifis, B. G. Hockley, et al., Cyclotron-Based Production of ⁶⁸Ga, [68Ga]GaCl₃, and [68Ga]Ga-PSMA-11 from a Liquid Target, EINMMI Radiopharm. Chem, 2020, 5(1), 1-18.
- 169 B. J. B. Nelson, J. Wilson, S. Richter, M. J. M. Duke, M. Wuest and F. Wuest, Taking cyclotron ⁶⁸Ga production to the next level: Expeditious solid target production of ⁶⁸Ga for preparation of radiotracers, Nucl. Med. Biol., 2020, 80, 24-31.
- 170 J. W. Engle, V. Lopez-Rodriguez, R. E. Gaspar-Carcamo, H. F. Valdovinos, M. Valle-Gonzalez, F. Trejo-Ballado, et al., Very high specific activity 66/68Ga from zinc targets for PET, Appl. Radiat. Isot., 2012, 70(8), 1792-1796.
- 171 S. Zeisler, A. Limoges, J. Kumlin, J. Siikanen and C. Hoehr, Fused Zinc Target for the Production of Gallium Radioisotopes, Instruments, 2019, 3(1), 10.
- 172 H. Thisgaard, J. Kumlin, N. Langkjær, J. Chua, B. Hook, M. Jensen, et al., Multi-curie production of gallium-68 on a biomedical cyclotron and automated radiolabelling of PSMA-11 and DOTATATE, EJNMMI Radiopharm. Chem, 2021, 6(1), 1-11.
- 173 J. Kumlin, J. H. Dam, C. J. Chua, S. Borjian, A. Kassaian, B. Hook, et al., Multi-Curie Production of Gallium-68 on a Biomedical Cyclotron, Eur. J. Nucl. Med. Mol. Imag., 2019, 46(suppl. 1, 1, SI), S39.
- 174 M. Enferadi, M. Sadeghi and H. Nadi, 72As, a powerful positron emitter for immunoimaging and receptor mapping: Study of the cyclotron production, Radiochemistry, 2011, 53(4), 407-410.

- 175 P. A. Ellison, F. Chen, T. E. Barnhart, R. J. Nickles, W. Cai and O. T. Dejesus, Production and isolation of ⁷²As from proton irradiation of enriched 72GeO2 for the development of targeted PET/MRI agents, in: Proceedings of the 15th International Workshop on Targetry and Target Chemistry. 2015.
- 176 M. Jennewein, M. Lewis, D. Zhao, E. Tsyganov, N. Slavine, J. He, et al., Vascular imaging of solid tumors in rats with a radioactive arsenic-labeled antibody that binds exposed phosphatidylserine, Clin. Cancer Res., 2008, 14(5), 1377-1385.
- 177 P. Ellison, F. Chen, S. Goel, T. Barnhart, R. Nickles, O. DeJesus, et al., Intrinsic and stable conjugation of thiolated mesoporous silica nanoparticles with radioarsenic, ACS Appl. Mater. Interfaces, 2017, 9(8), 6772-6781.
- 178 P. A. Ellison, T. E. Barnhart, F. Chen, H. Hong, Y. Zhang, C. P. Theuer, et al., High Yield Production and Radiochemical Isolation of Isotopically Pure Arsenic-72 and Novel Radioarsenic Labeling Strategies for the Development of Theranostic Radiopharmaceuticals, Bioconjugate Chem., 2016, 27(1), 179-188.
- 179 A. DeGraffenreid, Y. Feng, D. Wycoff, R. Morrow, M. Phipps, C. Cutler, et al., Dithiol aryl arsenic compounds as potential diagnostic and therapeutic radiopharmaceuticals, Inorg. Chem., 2016, 55(16), 8091-8098.
- 180 W. Ali. Evaluation of Nuclear Reaction Cross Sections Relevant to the Production of Emerging Diagnostic Radioisotopes Fe-52 and As-72. Government College University, Lahore, 2012.
- 181 I. Spahn, G. F. Steyn, F. M. Nortier, H. H. Coenen and S. M. Qaim, Excitation functions of natGe(p,xn)^{71,72,73,74}As reactions up to 100 MeV with a focus on the production of ⁷²As for medical and ⁷³As for environmental studies, Appl. Radiat. Isot., 2007, 65(9), 1057-1064.
- 182 Y. Li, S. F. Shen, J. H. Gu, S. H. Shi and J. Y. Liu, A study on the decay of ⁷²As, Chin. Phys., 2005, **14**, 487–493.
- 183 R. Guin, S. K. Das and S. K. Saha, Separation of carrier-free arsenic from germanium, J. Radioanal. Nucl. Chem., 1998, 227(1-2), 181-183.